Elevated-Temperature Deformation at Forming Rates of 10^{-2} to 10^2 s^{-1}

H.J. McQUEEN

In the hot working at constant strain rate ($\dot{\varepsilon}$) of Al and α Fe alloys at 0.5 to 0.9 T_M (absolute melting temperature), steady-state deformation is achieved in similarity to creep, which is usually at constant stress. After an initial strain-hardening transient, the flow stress becomes constant in association with a substructure which remains equiaxed and constant in the spacing of sub-boundaries and of dislocations in both walls and subgrains. All these spacings become larger at higher temperature (T) and lower $\dot{\varepsilon}$ values as well as with lower stress, being fully consistent with the relationships established in creep. Because hot working can proceed to a much higher true strain in torsion ($\sim$100) and compression ($\sim$2) as well as in extrusion ($\sim$20) and rolling ($\sim$5), it is possible to confirm that grains continue to elongate while the subgrains within them remain equiaxed and constant in size. When the thickness of grains reaches about 2 subgrain diameters (d_s), the grain boundaries with serrations ($\sim d_s$) begin to impinge and the grains pinch off, becoming somewhat indistinguishable from the subgrains; this has been called geometric dynamic recrystallization (DRX). In polycrystals as at 20 °C, deformation bands form and rotate during hot working according to the Taylor theory, developing textures very similar to those in cold working. In metals of lower dynamic recoverability such as Cu, Ni, and γ Fe, new grains nucleate and grow (discontinuous DRX), leading to a steady state related to frequently renewed equiaxed grains, containing an equiaxed substructure that develops to a constant character and defines the flow stress.

I. INTRODUCTION

THE objective of this article is to present the hot-working view of elevated-temperature deformation, which is gained from rates of 10^{-2} to 10^3 s^{-1} to true strains usually in excess of 1 (63 pct reduction) and up to 10 industrially and 100 in testing.[1-18] The fields of creep and hot working appear to be closely related, since they share similar temperature ranges and, hence, thermally activated mechanisms.[19] However, in addition to a much higher strain rate and somewhat higher temperature (which partially counteracts the former), hot shaping proceeds to much higher strains. Steady-state deformation, where the temperature (T), steady-state rate ($\dot{\varepsilon}_S$), and steady-state strength (σ_S) are constant, is usually attained at sufficient strain in both creep and hot working; however, in the former, it is T and σ which are usually held fixed, whereas in the latter it is T and $\dot{\varepsilon}$.

The same relationships between strain rate, stress, and temperature in steady-state deformation can be used for both parameters.[20-28] The high strain in hot working allows observation of mechanisms common to creep, namely, of dynamic recovery (DRV) of the dislocation substructure at a mature stage, to further elucidate its operation, and also of dynamic recrystallization (DRX), infrequent during creep. The fracture mechanisms are similar under both strain-rate regimes; but, at the higher rate, the ductility is usually greater because of the diminished proportion of intergranular sliding and may be enhanced by DRX or static recrystallization (SRX) between passes. The large strains due to compressive components in most primary forming processes considerably color the objectives of testing and the interpretation of results. Finally, the diverse objectives of specific material properties distinguish research activities in the two fields. In products such as sections, plates, extrusions, or forgings intended for direct service, the preservation of the hot-worked substructure, or the grain refinement from recrystallization, in combination with phase changes in thermomechanical processing (TMP), endows improved strength in application (Table I, Section VIII).[12-17]

There are considerable paradigm divergences between the two fields as a result of different industrial problems and training. The creep metallurgist has considerable professional skill in understanding the flow and rupture mechanisms, defining the creep conditions, and in specifying composition and heat treatment, being elated when an alloy deforms less and survives longer under more exacting conditions of temperature and stress.[29-40] On the other hand, the metal worker depends on experience to maintain high levels of production while reducing operating costs and scrap losses, becoming enthusiastic about an alloy which can be deformed extensively with low forces after a moderate preheating temperature. The creep metallurgist is concerned with the installation of parts free of defects and with microstructures which remain stable over the projected life, whereas the "blacksmith" is concerned with whether the cast material, with its columnar grains, segregation, and macrodefects, can be processed without too many rejects. Furthermore, control of the dimensions, shape, and surface quality are combined with concern for microstructural enhancement of product properties in TMP. As an example, advanced Ni-based superalloys with enhanced resistance to

Table I. TMP, Dispersoid Stabilized Alloys[14,15,98,157]

500 °C		Tension 20 °C					Torsion at $\varepsilon = 4$		
		Test*	Annealed**,†	Wire	Rod	200 °C	300 °C	400 °C	500 °C
Al	UTS MPa	120	130	212	145	145	115	75	40
0.5Fe	d_s μm	1.0	0.7	0.4	0.85	0.83	—	—	1.3
0.5Co	σ_y MPa	99	100	180	120	—	—	—	—
98 pct*	elongation	25 pct	18 pct	3 pct	18 pct	4.7	7.2	>20	>20
Al	UTS MPa	110	108	212	125	135	110	65	35
0.65Fe	d_s μm	1.7	1.4	0.6	1.0	1.0	1.1	2.9	6.8
	σ_y MPa	64	70	175	110	—	—	—	—
92 pct*	elongation	27 pct	26 pct	3 pct	20 pct	6.2	9.0	9.5	>20
Al (EC)	UTS MPa	62	—	173	110	105	80	45	25
99.7 pct	d_s μm	4.6	2.8	0.8	1.6	1.4	2.0	33	7.2
	σ_y MPa	35	50	160	96	—	—	—	—
71 pct*	elongation	25 pct	26 pct	2 pct	15 pct	—	—	—	—

*Stability after 2000 h, test at 180 °C.
**Continuous processed, 10 pct stronger than recrystallized rod.
†Annealed 290 °C 3 h for SRV only in order to raise ductility.
Moving from right to left: properties during hot, cold, recovery processing, leading to final TMP properties at left.

deformation at elevated temperatures are the application engineer's delight but the metal former's anguish, because of a very limited forging window. These paradigm divergencies result in communication gaps.

In the period from 1945 to 1970, great advances were made in creep with respect to observations of substructure dislocation mechanisms, grain-boundary sliding, migration and cracking, constitutive equations, and theoretical models. In the last decade of that period, these ideas were applied to hot working by approximately eight principal researchers (more than four publications in hot working); of these, half had experience in creep.[4,7,19] The most important aspects of hot working will be described briefly and compared and contrasted with results or concepts in creep in order to provide a deeper, broader perspective of high-temperature deformation. The topics include flow curves with steady-state regimes, constitutive equations with activation energies, substructure evolution with serration of grain boundaries (GBs), deformation bands and texture formation, dynamic recrystalization, and the influence of GB sliding on ductility and dynamic precipitation and coalescence. The selection of ideas and the emphasis on hot working are based on the author's long experience and are well documented so that creep researchers can access them. The author's comments on creep are based on scattered acquaintance and are not so well referenced; for this and his suggestions of areas where creep researchers could gain beneficial insights, he apologizes for his limitations.

II. MACROSCOPIC MECHANICAL BEHAVIOR

In metal-forming processes, the control parameters of temperature, strain rate ($\dot{\varepsilon}$) and strain (ε) are quite variable in both time and space because of machinery behavior (*e.g.*, the forging hammer), tooling geometry (*e.g.*, the roll curvature), and die chilling and friction.[13–15,41–45] To establish the precise relationships of the three variables and their influence on flow stress (σ) and microstructure, it is common to test with T and $\dot{\varepsilon}$ constant (Figure 1(a)).[2–6,46,47] In combination with shear-line calculations or finite-element methods

(FEMs), such relationships make possible process analysis.[13,41–44] Industrial hot forming is frequently applied in multiple stages,[44,45,47] as is also common in creep service, but the significantly different behavior during the intervals is thoroughly examined later. In creep service, the load and T are normally constant, although there are excursions away from that due to fluctuations in service demands. Again, it is customary to creep test at constant T and σ values to facilitate scientific analysis;[29–40] the data may be presented as $\dot{\varepsilon}$-ε curves, since that better parallels the σ-ε curves. Constant-strain-rate tests are sometimes used, and the relationship between the two has been shown by Blum *et al.*;[48,49] for simplicity, this presentation will focus on constant-σ creep.

The σ-ε curves for hot working are generally carried out to high strains, as in shaping operations,[1–12] and, thus, are conducted in compression (<2 to 5)[2,50,51] or torsion (Figure 1) (<100, the von Mises equivalent strain),[2,46,52–57] thus avoiding the tensile necking due to diminishing strain hardening ($\theta = d\sigma/d\varepsilon$). For Al, α Fe, and other bcc metals, the flow curves exhibit declining strain hardening to attain at ε_S (lower for higher T or lower $\dot{\varepsilon}$ values) a steady-state regime due to DRV (Figure 1(a)).[3–12,18,20–23,27,28,52–58] The plateaus frequently diminish to varying degrees depending on the microstructural evolution, such as particle coalescence or deformation heating mitigated by heat loss. In Cu, Ni, and γ Fe, the curves exhibit a sharp initial peak followed by work softening due to the first wave of DRX (Figure 1(b)).[3–11,16–18,59–64] In creep, tension is usually employed in a way similar to service situations and because of the availability of accurate extensometers.[31–39,65] In creep, $\dot{\varepsilon}$ drops rapidly as the mobile dislocation density declines, due to exhaustion of easy dislocation movement (equivalent to strain hardening), to attain a steady-state regime ($\dot{\varepsilon}_S$) due to DRV at ε_S, usually much less than in hot working.[3–5,21,26,51] Exceptionally in pure Cu or Ni, there are sudden excursions of rapid straining due to DRX followed by $\dot{\varepsilon}$ transients, as in initial loading.[66,67] The steady-state regimes are often rather short, due either to necking or to initiation of internal fissure formation; in severe cases, the minimum creep rate
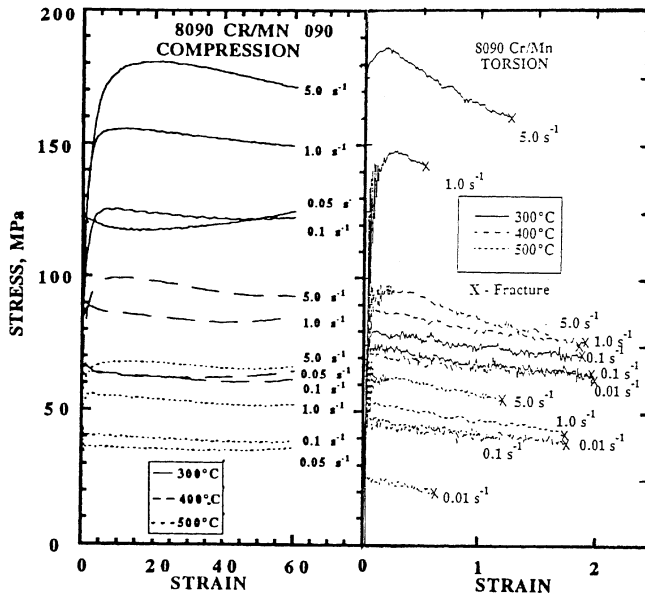
(a)
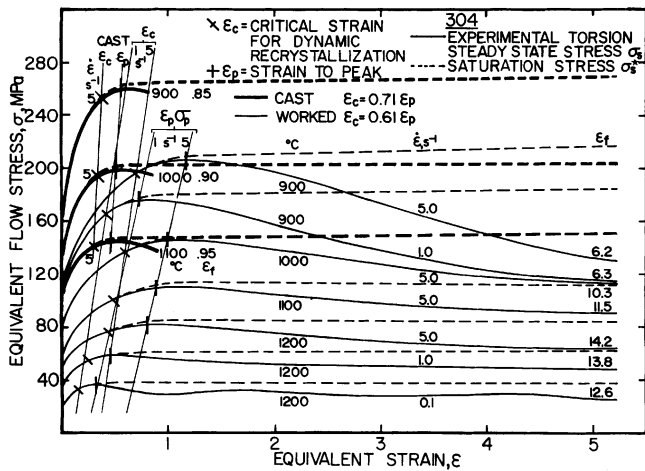
(b)

Fig. 1—Representative flow curves for (*a*) 8090/Cr/Mn (Al-Li-Mg-Cu) from compression to $\varepsilon = 0.6$ and torsion to $\varepsilon = 2$; DRV with softening due to particle coarsening.[170] (*b*) 304 (Fe-Cr-Ni) both as-cast C with segregated ferrite and worked-homogenized W; the softer ferrite particles raise strain hardening θ and σ_p but lower ε_p by PSN-DRX (σ_s*, Fig. 5).[76]

(ε_{min}) may actually be higher than the true ε_S level.[37–39,48,49] Compression testing at a constant σ value not only establishes $\dot{\varepsilon}_S$ accurately, but points on the $\dot{\varepsilon}$-ε curves can be correlated to these on flow curves at a constant $\dot{\varepsilon}$ level.[48,49] For the same material, the hot-work steady state (constant σ_S at T and $\dot{\varepsilon}_S$) is the same as the creep steady state (constant $\dot{\varepsilon}_S$ at T and σ_S).[19–23,27,28]

Constitutive equations are significant in hot working for modeling processes and permit extrapolation to strain rates beyond the test capabilities. The constitutive equations in creep are beneficial for predicting creep rates at stresses lower than those tested, because of the excessive time that would be required; however, due to failure mechanisms different from that of flow, they may not predict the creep life. The constitutive equations employed for hot working[3,9,16–19,57–59,62–64,68–70] and creep[20–40,65] include the following:

$$A_P \sigma^{n_p} = \dot{\varepsilon} \exp (Q_P/RT) = Z_P \text{ (power)} \qquad [1]$$

$$A_G (\sigma/G)^{n_g} = \dot{\varepsilon} \, kT/(\mathbf{b}GD_0 \exp (-Q_D/RT) \qquad [2]$$

$$A_E \exp \beta\sigma = \dot{\varepsilon} \exp (Q_E/RT) = Z_E \text{ (exponential)} \qquad [3]$$

$$A (\sinh \alpha\sigma)^n = \dot{\varepsilon} \exp (Q/RT) = Z \text{ (sin } h) \qquad [4]$$

where $A_P, A_G, A_E, A, \alpha, \beta, n_p, n_g, n_s, D_0, Q_P, Q_D, Q_E,$ and Q are empirical material constants, R is the gas constant, k is the Boltzman constant, $\mathbf{b}$ is the Burgers vector, and G is the shear modulus (Figures 2 and 3). The various A, n, and Q parameters, while being roughly equal, may differ for the same set of data, for results from different compositions or microstructures of the same alloy and for the same material determined in different T or $\dot{\varepsilon}$ ranges of hot working or creep.[57,68] The Zener–Hollomon parameter Z is particularly beneficial in hot working, since it embraces the two control variables. For hot working of alloys with DRV, σ refers to the steady-state value (σ_S and Q_{HW}), the maximum value if the plateau diminishes slightly, or σ at a fixed high strain if friction prevents a plateau. For alloys with DRX, σ may relate to the peak σ_P level or to the start of steady state (σ_S) after work softening, which is much greater at high Z values, resulting in Q_S (σ_S) being much less than Q_{HW} (σ_P).[62–68]

In creep, the power law is preferred; however, at higher stress levels, n_p varies with stress, becoming larger in the domain referred to as power-law breakdown, into which hot-working conditions generally fall (Figures 2(a) and (b)).[20–28] For alloys containing particles, the power law is suitable only if a threshold stress to release dislocations is subtracted from the applied stress. The activation energy for creep (Q_P) is generally similar to that for self-diffusion (Q_D), indicating that dislocation climb is rate controlling due to its dependence on vacancy migration; the n_p values are near 4.5. The n_p values are near 3 in some solute alloys, indicating that rate-controlling dislocation motion is dependent on the dragging of Cottrell atmospheres with Q_D for the solute atoms. In Al-Mg alloys, the Q_D value for Mg in Al is similar to that for Al itself.[20–28,35–38] In a project involving both hot torsion to $\varepsilon = 4$ and compression creep to $\varepsilon = 1.5$ of Al, Al-11Zn, Al-5Mg, Al-5Mg-0.7Mn, and Al-1Mn with the same impurities, the data fitted consistently to both Eqs. [1] and [2] with regions of power-law breakdown and of power law, with $n_p = 4.5$ for alloys without Mg with $n_p = 3$ for alloys with Mg (Figure 4).[20–28] There was a divergence from power law at low stress for alloys with Al_6Mn particles, due to threshold effects. The similarity of Q for creep and hot working of Al has been confirmed over 15 orders of magnitude in the Z value.[70] Similar correlations of data for ferritic stainless steel and for austenitic stainless steel include both creep and hot-working values.[40]

The sinh law of Eq. [4] is preferred in hot working since it is usually linear over a broad range when $\alpha \approx \beta/n_p$, since it approximates Eq. [1] at low σ levels and Eq. [3] at high σ levels (the opposite σ levels for which those functions show curvature), as shown in Figures 2(a) and (b) and 3.[68,69] The suitable values of α have been found to be near 0.052 MPa^{-1} for Al alloys and composites,[57,68,70] near 0.014 MPa^{-1} for ferritic and C steels,[17,68] and near 0.012 MPa^{-1} for austenitic stainless, high-strength low-alloy, and tool steels.[17,62–64,68,69,71] These values have been determined through application to many alloys and also through variations of α for optimization. The values of n vary inversely
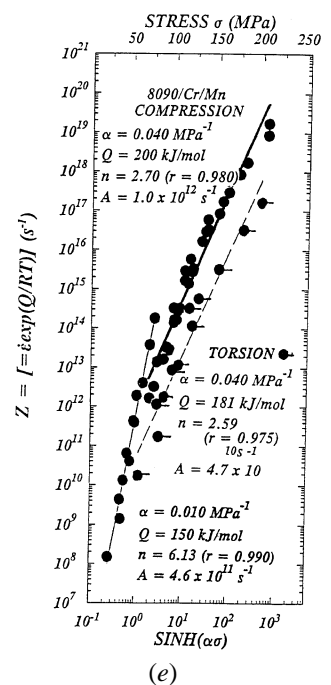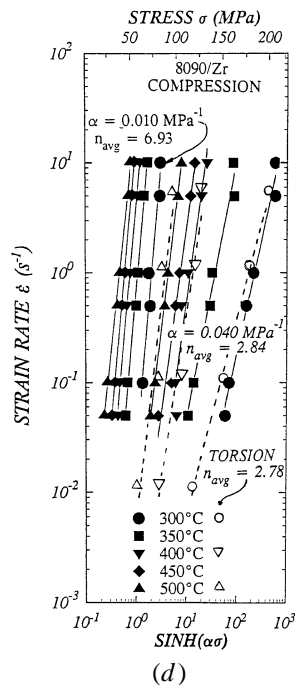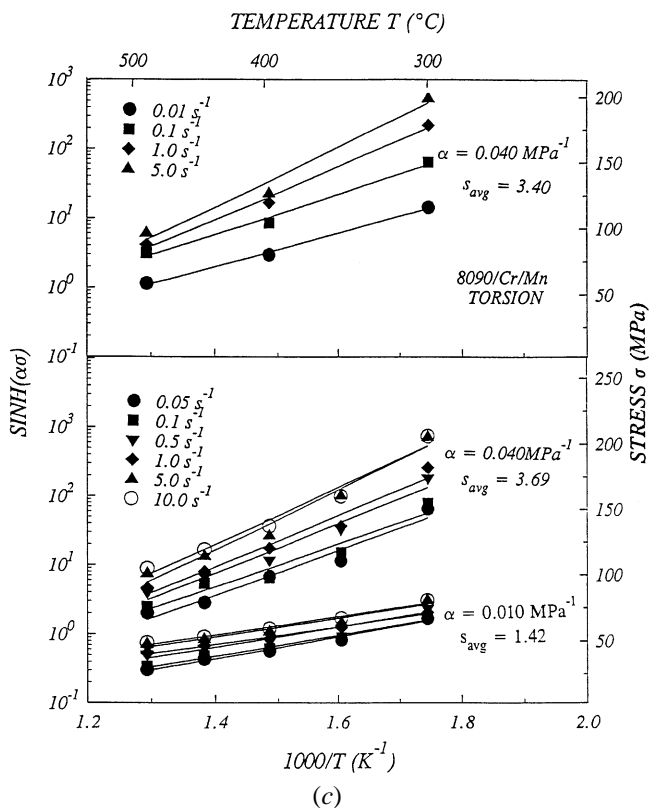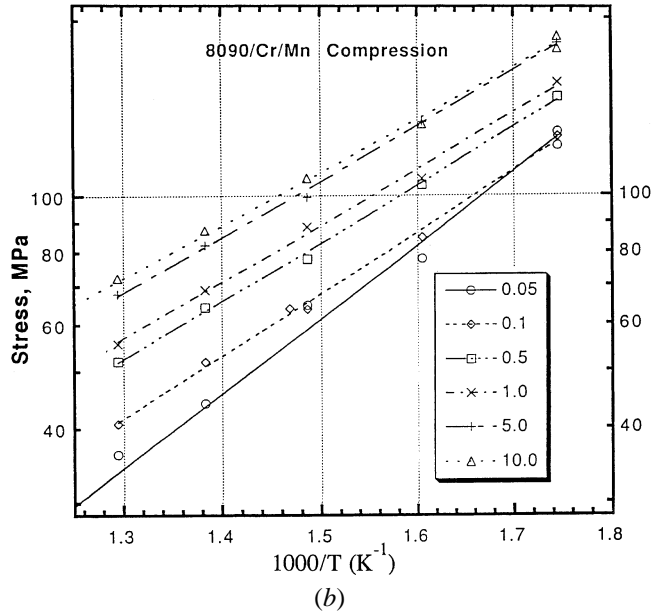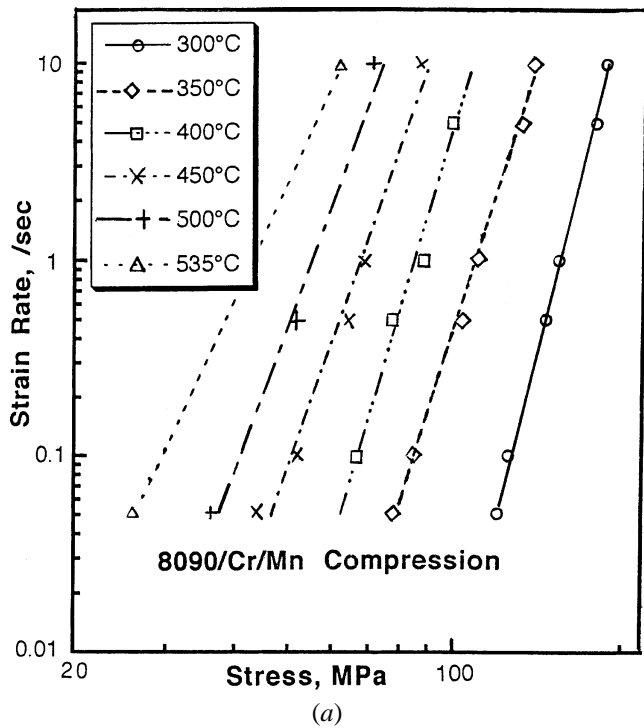
Fig. 2—Constitutive analyses for compression and torsion of 8090/Cr/Mn: (a) and (b) power law and (c) and (d) sinh law (α = 0.04 MPa^{-1}) show close agreement. (e) Plot of data according to sinh law and Zener–Hollomon parameter compression and torsion. Best fit for α = 0.01 MPa^{-1} but stable Q_{HW} for 0.04 to 0.08 MPa^{-1}.[170]

with α. For the optimum values of α, the n values are generally lower than the equivalent n_p values. The n values are generally lower for solute-drag alloys, but are also so for other strong alloys. For Al alloys, the Q_{HW} values generally increase as the alloy content increases and also as the impu-

rity content rises.[57,68,72] This rise is not associated with any fundamental change in mechanism, as confirmed by microscopic examination; the rise in Q_{HW} may be attributed to additional retardation in DRV caused by particles or other obstacles.[68,72]
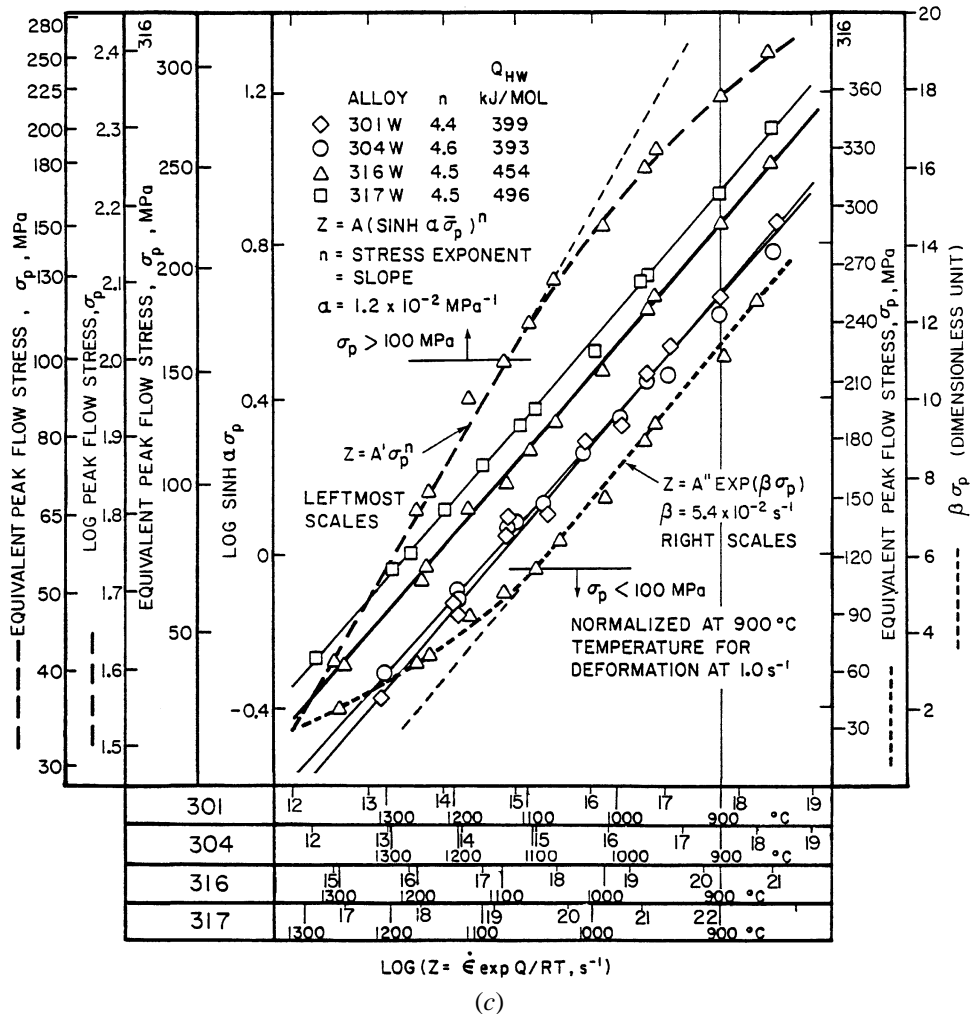
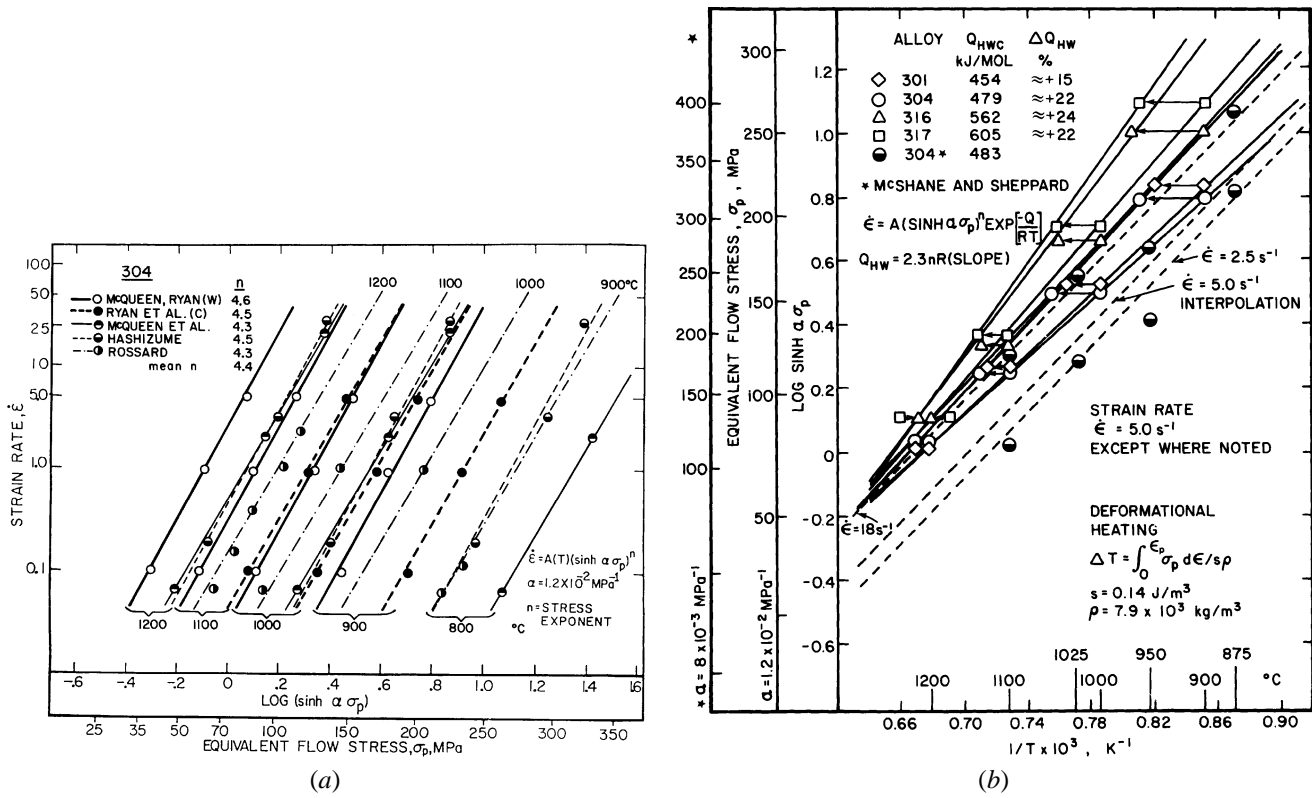Fig. 3—Constitutive analysis by sinh law for 304 W with some 304C showing greater strengths: (a) log $\dot{\varepsilon}$ vs log (sinh $\alpha\sigma$) compared to other compositions; (b) log (sinh $\alpha\sigma$) vs (1/T) with heating correction compared to 316 and 317; and (c) Z vs sinh $\alpha\sigma$ with log σ and exp $\beta\sigma$ showing the failure of fit at high and low σ, respectively.[62–64,69,76]
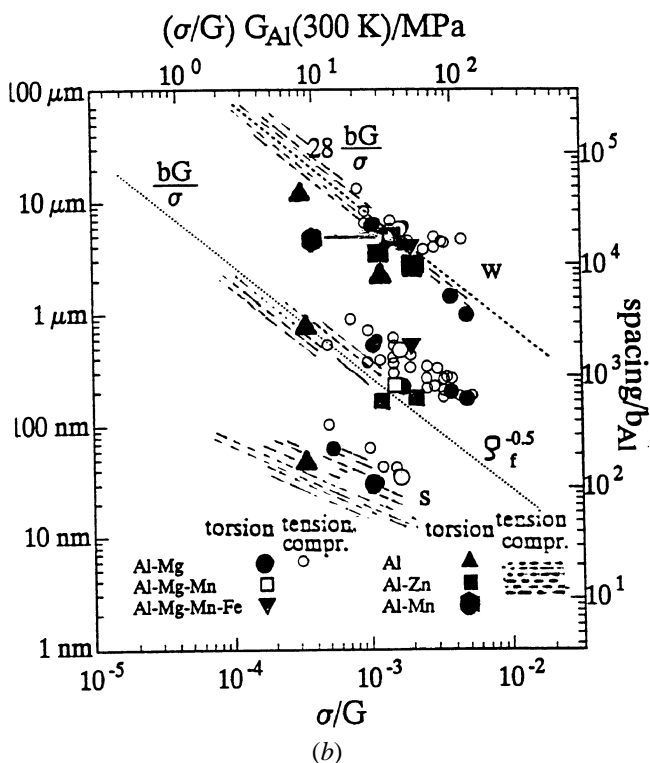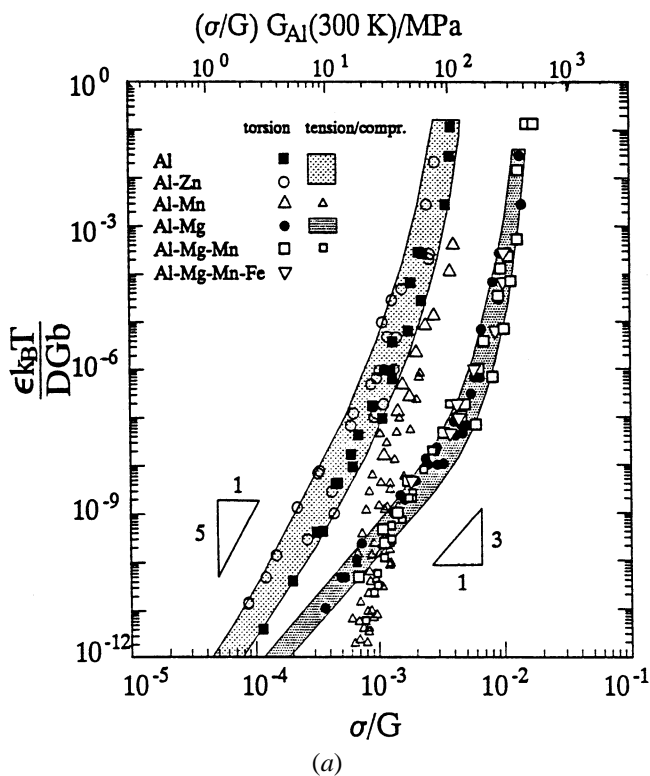
(a)

(b)

Fig. 4—Data from torsion tests to $\varepsilon = 4$ on solute and dispersoid Al alloys compared to creep results on *(a)* strain rate normalized by diffusion coefficient ($\sim$145 kJ/mol for both Al and Mg atoms) against stress normalized by shear modulus and *(b)* spacings of sub-boundaries w ($\approx d_s$) and of dislocations both internal $\rho_i^{-0.5}$ and walls s_w (dotted bands for Al and Al-Zn in creep).[20–24]

For alloys undergoing DRX, the values of Q_{HW} associated with σ_P rise with alloy content, for example, in austenitic stainless steel with a solute or α particle content,

because σ_P rises as T declines, not only because of increased strain hardening (reduced DRV), but also because ε_P rises.[3–5,16–18,59–64,68] The Q_{HW} values are considerably higher than those for creep of equivalent alloys. The Q_S values are not the activation energy for DRX, although that is sometimes inferred, since they are associated with the steady state due to DRX.[62–64,68] The rate of the first wave of DRX has been determined; the activation energy is much less than Q_S and is similar to that for grain-boundary migration.[64] To sum up, the sinh constitutive equation is valued because it is effective for modeling.[13,43] The values of n and of Q_{HW} vary in a suitable manner with alloy content, but are not well related to the values determined in creep; however, as shown for Al alloys, there is the possibility of correlating creep and hot working through Eq. [2].[20–28,40]

A constitutive analysis based on the decrease of θ with σ as ε rises to the steady state, provides analysis of dynamic-recovery evolution with ε, $\dot{\varepsilon}$ and T, primarily in Al alloys;[73,74,75] similar analysis can be made from plots of $d \ln \dot{\varepsilon}/d\varepsilon$. Austenitic stainless steel[62,63,76] and tool steels[71] have been subjected to mathematical analysis, providing activation energies at high T values similar to those from the sinh equation (Figure 5). The analysis has also provided an accurate determination of the critical strain for DRX, clarifying the kinetic analysis.[62,63,76]

III. DISLOCATION SUBSTRUCTURE

The flow-stress reduction and ductility improvement in hot working is clearly due to the thermal activation of dislocation cross slip and climb. In the period from 1955 to 1970, much was learned by hot workers[4,7] from creep research and theories, since this field had reached much greater maturity in terms of numbers and long experience of the researchers.[30–34] Work on pure metals and simple alloys encouraged this, since the microstructures of more complex alloys tend to be quite different in hot working and in creep. While DRV with subgrain formation produces most of the softening in both high and low stacking-fault-energy (SFE) metals (Figures 6 through 8), the substructure density in the latter becomes sufficient to nucleate new grains and cause an additional reduction of about 20 pct from the peak stress.[1–11] Discontinuous DRX has been found in Al and α Fe only when the purity exceeds 99.999 pct (in the former, SRX occurs at 20 °C).[24,77–80] In Al and α Fe, the dislocation density is augmented, in the form of tangles with rising polygonization, until subgrains of stable size (d_s) are formed at the beginning of the steady-state regime.[81,82]

Al has been strained to high degrees in rolling (>2.3), in extrusion (>3.4), and in torsion (>100), during which the subgrains remain constant in size and equiaxed (Figure 6).[4,5,11,12,18,20–27,42,44,45,51,58,72] For this behavior, it provides stronger confirmation than creep, where the extent of steady state is often very limited. This mechanism has been named "repolygonization"[83] and proceeds by the migration, partial disintegration, and reknitting of the subgrain boundaries (SGBs),[4,12,52–56] as observed in detailed creep studies, notably during *in-situ* deformation in high-voltage transmission electron microscopy (TEM).[84,85,86] The spacing of the SGB is maintained constant by the internal stress fields. In addition to the aforementioned features, the misorientations (φ) of the SGBs have been shown to be constant up to strains
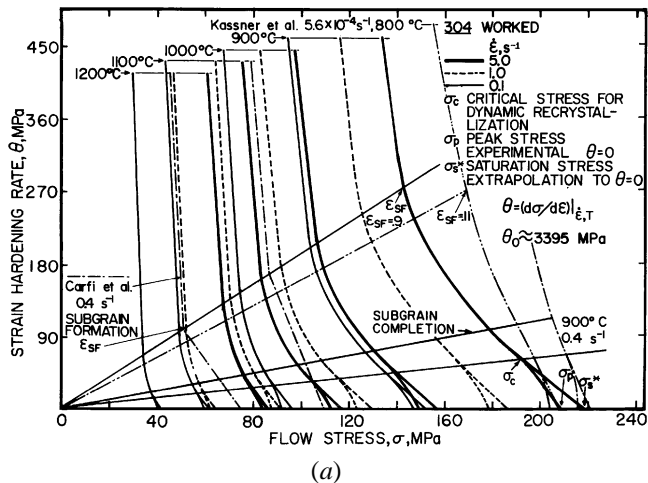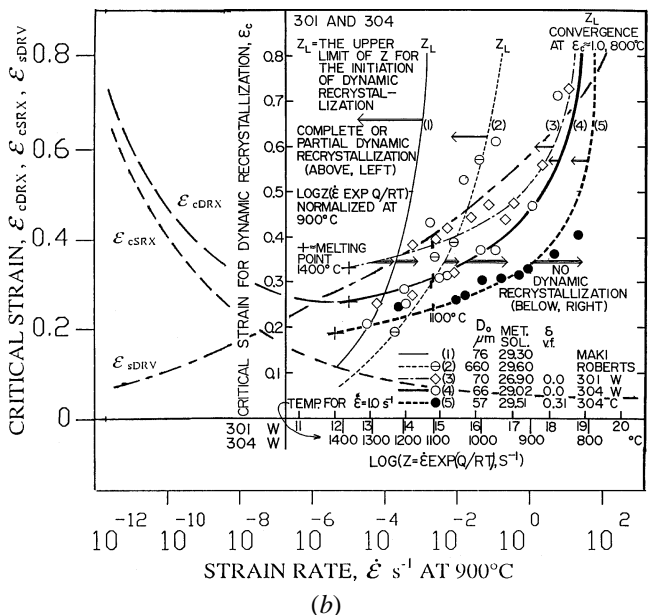
Fig. 5—Constitutive analysis for 304 according to Kocks–Mecking theory: (a) θ vs σ to find σ_s^* (Fig. 1); a downward inflection in the curve toward σ_p ($\theta = 0$) marks nucleation at σ_c (ε_c);[76] (b) the dependence of ε_{cDRX} on Z (or $\dot{\varepsilon}$ at 1200 °C) for 304 and 301 (normalization explained[171]) with schematic lines for variation of ε_{sDRV} and ε_{cSRX} with $\dot{\varepsilon}$.[61,66,126,132]

Z in many hot-working experiments and the flow stress σ_S to be related to d_s:[3–5,9,51,62–65,76–79,83,90–92]

$$d_s = a + b' \log Z \qquad [5]$$

$$\sigma_s = c + e\, d_s^{-1} \qquad [6]$$

where a, b', c, and e are empirical constants. Creep results were added to the compilations for Al alloys and ferritic steels and were found to correlate well (Figure 10).[4,18–23,27,28,51,63,64,91–93] Blum and colleagues have made extensive correlations showing that the spacings of the SGBs ($w = d_s$), of the dislocations in the walls ($s_w \approx \mathbf{b}/\Psi$), and of those within the subgrains ($\rho_i^{-1/2}$) for Al, ferritic and austenitic steels are inversely proportional to σ_s/G.[21–28,40] The relationships of Eqs. [6] and [7] are overly simplified, since strength also depends on the dislocation network within the subgrains, for which the density (ρ_i) rises as d_s decreases.[21,39] In distinction from creep, hot working yields a product of which the strength is important. The yield stress (σ_y) or hardness at 20 °C was shown to depend on the subgrain size:

$$\sigma_y = \sigma_0 + k d_s^{-1} \qquad [7]$$

where σ_0 is the strength without substructure, and k is the strengthening coefficient.[93] The power of -1 differs from that of $-1/2$ in the Hall–Petch relationship for grains, because the obstacle effectiveness of the SGB varies with d_s, whereas that of the grain boundaries is independent of grain size.[14,15,93]

Hot working of Al-Mg alloys has helped to clarify that subgrains form during the steady state. Many creep reports maintained that solute drag, which restricted dislocation mobility, creating an inverted transient, inhibited subgrain formation.[32–35] However, subgrains were observed after hot working[3,4,12,72,94] and in creep.[37–40] McQueen and Kassner (with advice from Langdon) concluded that creep tests had commonly been halted as soon as $\dot{\varepsilon}_{min}$ was reached and showed that subgrains remained equiaxed with constant φ and d_s levels (Figure 9).[56,79,87–89,95] Efforts of a team under Blum and McQueen showed that, for the same Z value, the TEM subgrains in Al-5Mg formed gradually by $2\varepsilon_s$ (mechanical), with TEM d_s values being about one-fifth that in Al (σ_s being about 5 times higher), but with POM subgrains approximately equal and with the serrations becoming so billowing that they pinched off into separated crystallites.[21–28,96] These have been mistaken for DRX nuclei, but they do not grow because there is no differential in dislocation density.[79,80,97] The addition of fine particles to Al pins the substructure, limiting the subgrain size to the interparticle spacing at low T values, but at high T values, the dislocations climb around the particles with only a minor reduction in subgrain size.[3,4,26,90,98] Mg-Al alloys also exhibit solute drag, but, because of twinning, have many more inhomogeneous substructures and lower ductility.[48,49,99,100]

There are similarities of cold and hot working; the cells are usually elongated and much smaller than the subgrains yet, at high $\dot{\varepsilon}$ levels in stage III or IV, often become considerably polygonized.[25,26,101–108] The flow stress has been related to bowing out of dislocations from the walls and, thus, to their spacing (s_w) or link length.[99,101,108] These concepts have given support to Blum's composite model of creep, in which there are hard regions (SGBs) and soft subgrain interiors.[20,21,38–40] The strain in both regions is the

of 16 (Figure 9).[54,55,56] Another related phenomenon is the serration of the GBs as they migrate to absorb the dislocation arrays in SGBs; the wave length is about $2d_s$ and the amplitude is about $d_s/2$.[23,27,28,87–89] While polarized optical microscopy (POM) allows examination of a large field of subgrains, serrations, and differently oriented deformation bands in grains, it does not show the smaller subgrains, so the size is bigger than in TEM. Misorientations cannot be determined, the shading being related to polarizer angle.[52,53] Scanning electron microscopy with back-scattered electrons (SEM-EBS) reveals the subgrains which correspond well with POM and are usually larger than in TEM; misorientations (ψ) can be measured, but not those of the smallest subgrains with low ψ levels.[20,23,26,27] In TEM, all SGBs can be observed, and both ψ and the dislocation spacing (s_w) and arrangement in SGBs can be observed.

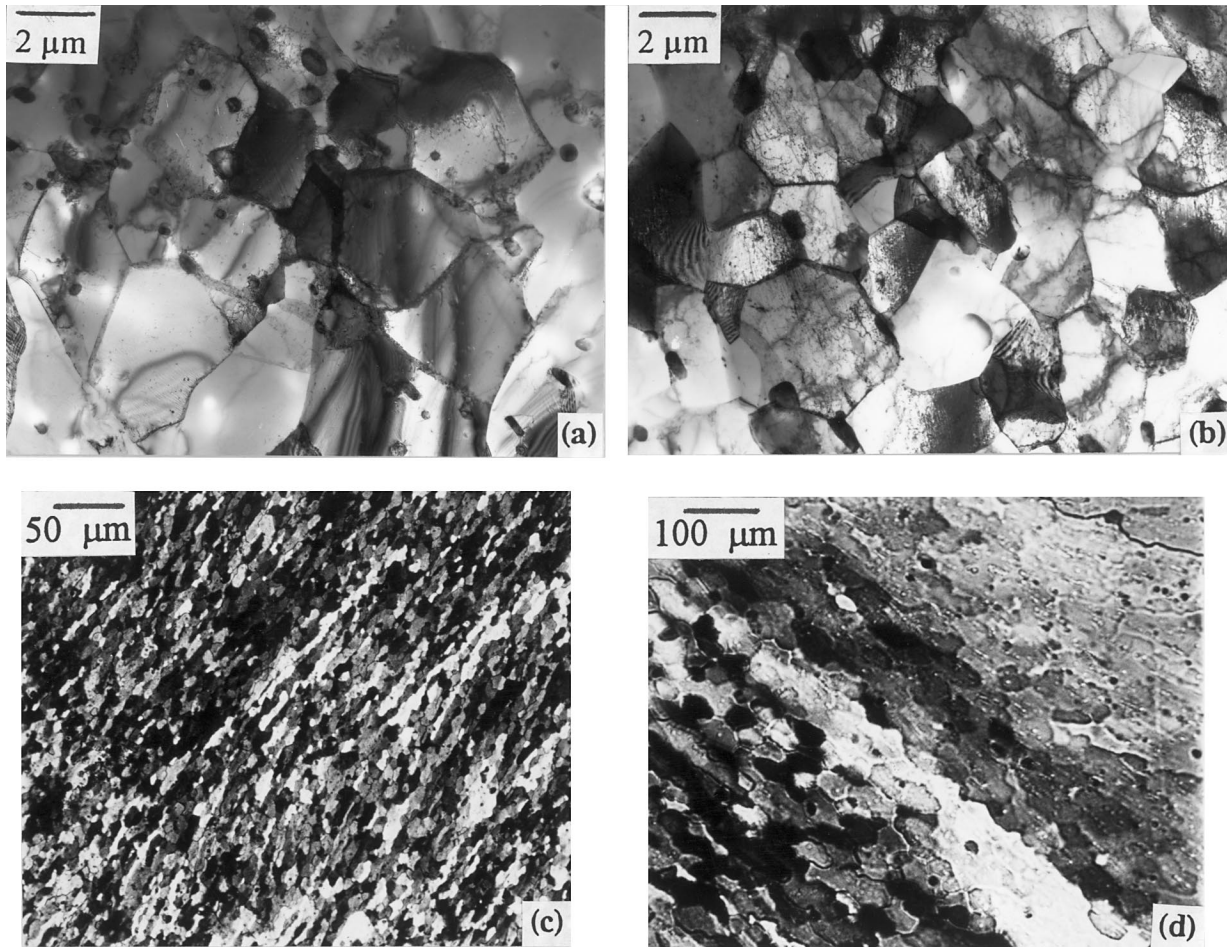The subgrain size d_s has been shown to be dependent on

Fig. 6—Subgrains in Al-0.65Fe to $\varepsilon = 4$ (*a* and *b*) with size and perfection decreasing from (a) 500 °C, 0.1 s^1, where Al$_3$Fe particles are visible inside the subgrains, to (b) 200 °C, 0.1 s^{-1} with particles pinning the sub-boundaries that hide them; and in (*c*) and (*d*) Al to $\varepsilon = 40$ at 400 °C, 0.2 s^{-1} observed by polarized optical microscopy (POM): (*c*) 100 μm grains barely discernible, subgrains emphasized, and (*d*) 2 mm grains with serrated GB and different contrasts; in both (*c*) and (*d*) equiaxed subgrains similar to (a) observed by TEM and SEM-EBSP (Fig. 10). (a) and (b) Ref. 98 and (c) and (d) Refs. 52 and 53.

same with dislocations, being assisted through the hard SGB by a large forward residual stress and being slowed by a residual backstress while speeding across the subgrains. The model also applies to Al-Mg alloys in which a solute friction stress must be included.[21,23,27,28,109] When the experimental spacings $w (= 0.64\, d_s)$, $\rho_i^{-0.5}$, and s_w are specified, the model can predict the transient and the values of ε_s and σ_s for Al and Al-5Mg. There are, of course, many eminent members of both the creep and hot-working community who do not accept the composite model;[37] the rate-controlling micro-structural feature is the dislocation network inside the sub-grains, which is the internal dislocation density (ρ_i).[30,31,33,37] However, in steady-state deformation, a vast collection of data for Al alloys, ferritic steels, and austentic stainless steels show that w, $\rho_i^{-0.5}$, and s_w are similarly dependent on σ_s/G and, hence, on each other.[21,38–40] Kassner and colleagues have increased ρ_i independently of d_s, so that it became a more important determinant of strength.[37,110]

The hot workability of austentic stainless steels is important to the industry, since they exhibit considerably higher strengths and lower ductilities than C steels in the austenite condition. However, they are also significant as a means to examine the substructure which is lost by the transformation of the C steel.[16,17,59,62–64,76,91,92,111,112] The correspondence is affected by the lower SFE and the solute effects. Substructures before the peak and in the DRX steady state were found to be related to stress in the same manner, which is consistent with the average dislocation density in the recrystallized grains defining strength. When the sizes were compared with creep results, they were found to be consistent with high-temperature results, but not with low-temperature creep data, which had a steeper slope.[63] Blum has been able to show the parallel dependence of the spacings w, $\rho_i^{-0.5}$, and s_w on σ_s/G for many grades and incorporated hot-working data.[40]

Aluminum and α Fe exhibit ultrahigh strains (>50) in torsion; this results in the grains becoming very elongated as helicoids wound around the axis.[18,21,27,28,52–56,111–114] Such straining proceeds with equiaxed subgrains and serrations of constant size until the thickness of the grain reaches about $2\, d_s$. The serrations on neighboring GBs begin to impinge, causing the grains to pinch off (become perforated in three dimensions) into shorter grains; this formation of refined grains containing a DRV substructure has been called geometric DRX (Figures 6(c) and (d)).[21–28,52–56,113,114] The outcome is that many subgrain facets become high-ψ ones derived from the original boundaries or from transition boundaries (next paragraph). This mechanism proceeds at
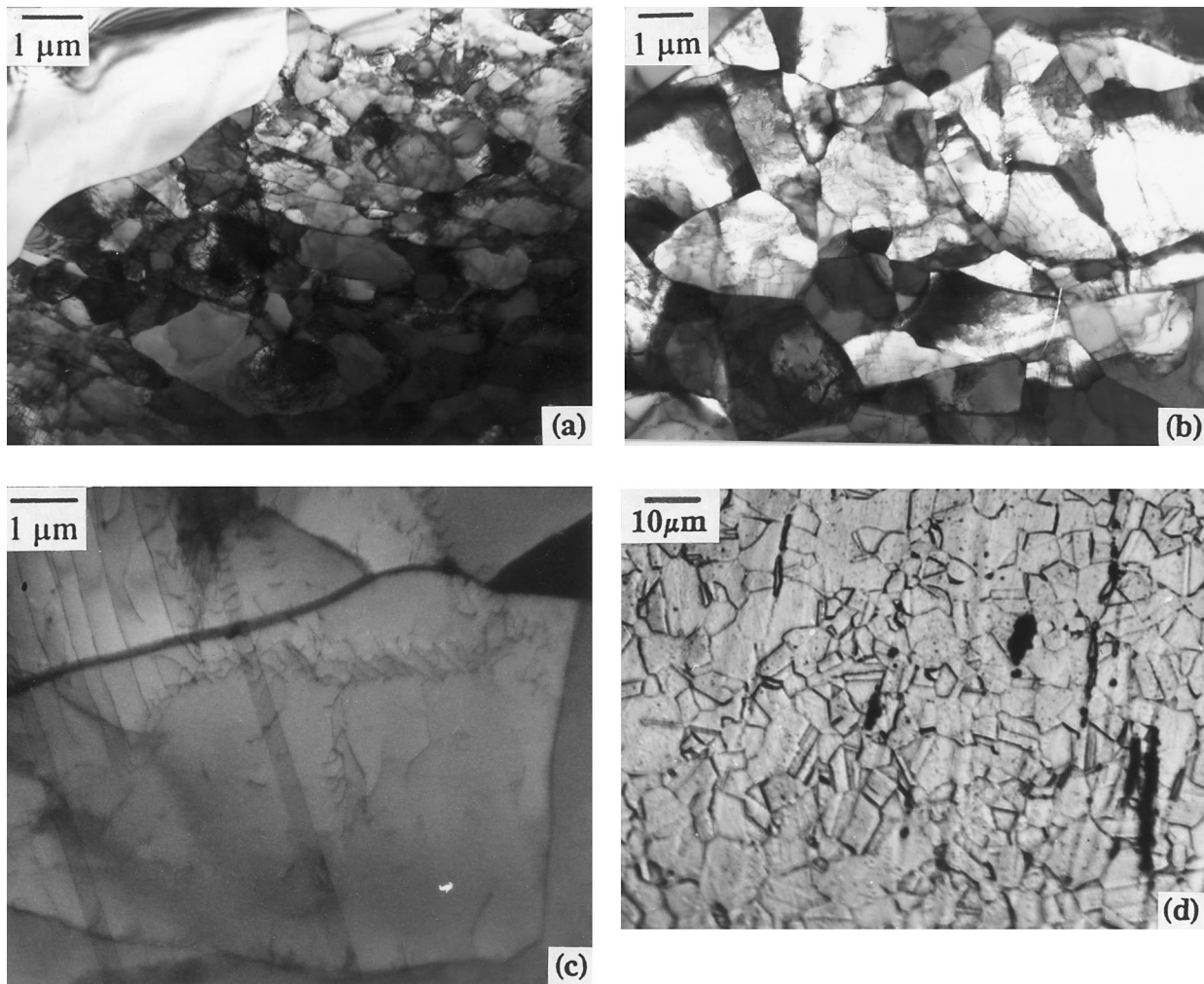
Fig. 7—Subgrains within dynamically recrystallized grains in 317 stainless steel: (*a*) 900 °C, 4 s^{-1} with two SRX grains; (*b*) 900 °C, 0.1 s^{-1}; (*c*) 1200 °C, 0.1 s^{-1}; and (*d*) 1000 °C, 1 s^{-1} DRX grains observed optically.[62,64]

lower ε levels as the initial grain size becomes smaller and as Z decreases because the subgrains are larger. The pinching-off process actually starts at low strains in the sharp grains at triple junctions.[21–26,80] The billowing serrations and pinched-off crystallites enhance the geometric DRX; moreover, the serrations are not permanent but rearrange as SGBs migrate, unravel, and reknit in new locations (constant d_s).[25–27,87–89] There is net migration of GBs into the grains with a finer substructure, which depends on their orientation.[25,26,80,113] The result is that a texture develops which has a markedly low Taylor factor, causing a strain softening of 10 to 20 pct at ε values of 4 to 20.[55,113]

After the foregoing emphasis on substructure, the formation of deformation bands in polycrystalline alloys must be considered.[115–121] In Taylor theory, a grain subjected to arbitrary deformation, as specified by five components of the stress tensor, must slip on as many systems; this can be reduced to three principal ones, with two of these playing a minor role. Grains with different orientations in the stereographic triangle slip on different sets of systems, causing lattice rotations that lead to texture formation dependent on the deformation mode.[102–106,115–121] Grains with certain orientations subdivide during initial straining into bands slipping on equivalent symmetric systems, which rotate in differ-

ent directions. The transition boundaries (TBs) between the bands increase in ψ as ε rises and are persistent, *i.e.*, not undergoing repolygonization.[24–26,80,121,122] At high T levels, the TBs appear similar in TEM to SGBs until diffraction confirms their nature; at 20 °C, they consist of several layers of very fine cells with accumulated $\psi > 35$ deg.[119] The deformation bands elongate like the grains, so that TBs align like original GBs and develop serrations. The deformation bands do not subdivide with the formation of block walls, as occurs in cold working, due partly to reduced Taylor constraints from factors that include GB sliding and additional slip systems.[24–26,80,121,122] There is also the process of repolygonization, which leads to complete rearrangement of the substructure in a strain increment about equal to the initial strain-hardening transient.[4,12,52–56,83,87,88] In consequence, when slip starts on a new system due to lattice rotation, microbands and dense dislocation walls do not form as in cold working.[102,106] Moreover, the scale of the substructure is markedly different compared to 5 μm subgrains in hot working: the cells in cold working are less than 1 μm and the blocks are about 5 μm in size.[24,25,26]

From SEM-EBS examination combined with orientation image mapping, the hot-worked substructure, notably at higher Z levels, exhibits some high-ψ transition boundaries;
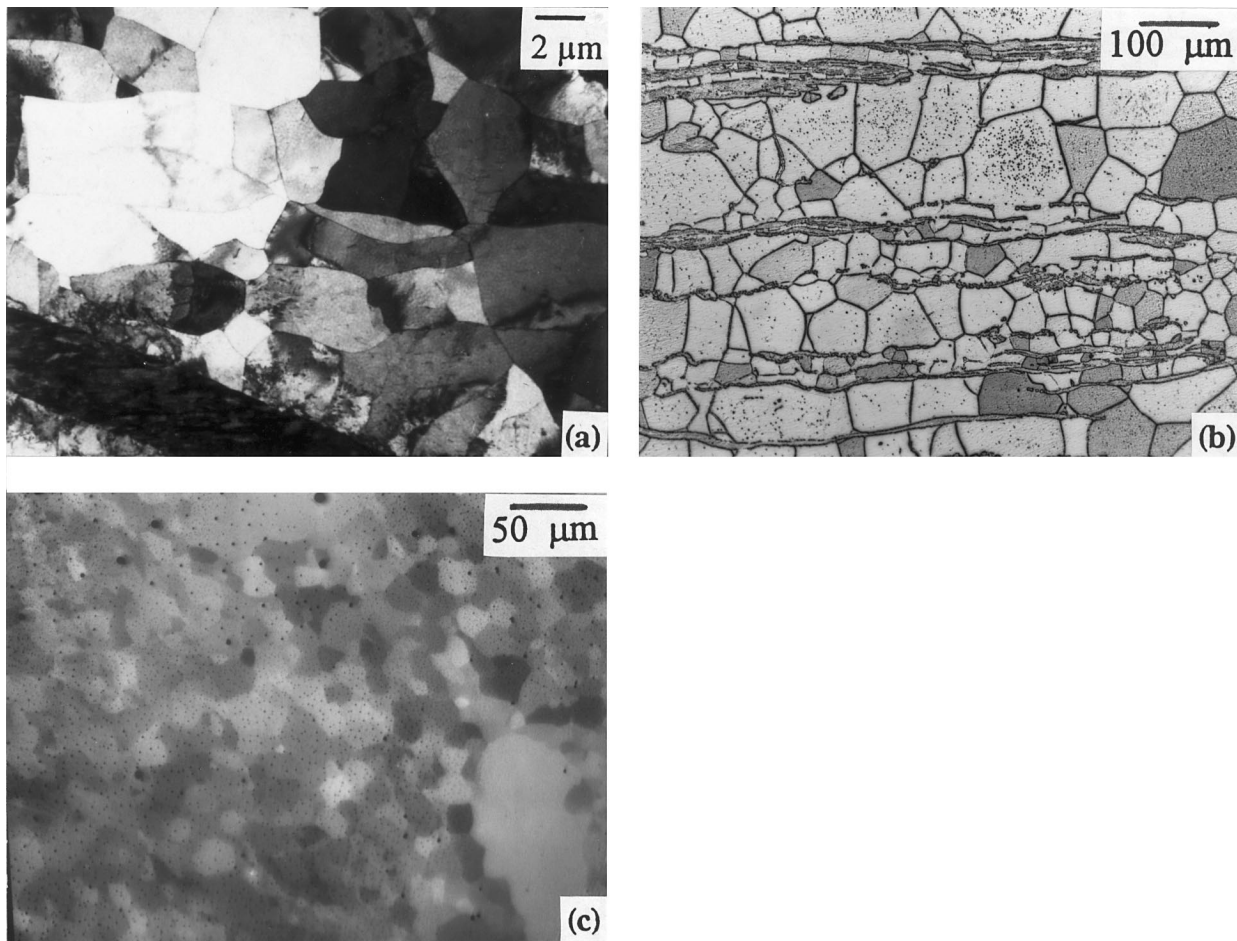
Fig. 8—Subgrains in as-cast ferritic stainless: (a) 430, 800 °C, 1 s^{-1} with austenite stringer exhibiting dense substructure, (b) 434, 1000 °C, 1 s^{-1} sizes vary in different grains separated by γ stringers, and (c) 409, 900 °C, 4 s^{-1} SEM-EBS.[111,112]

however, there are often short segments, *i.e.*, subgrain facets with $\psi > 10$ deg.[123–125] This is not surprising; in Al, the flow stress changes continuously from cold working to warm working from 100 °C to 300 °C (0.4 to 0.6 T_m), to hot working at temperatures >300 °C at $\dot{\varepsilon} = 1$ and to a creep equivalent of either $\dot{\varepsilon} < 10^{-4}$s^{-1} or $T > 500$ °C (0.83 T_m).[18,24–26] Hence, one must expect, for a declining T sequence, a continuous gradation in substructure density, with repolygonization becoming less perfect in the warm-working regime and some high-ψ SGBs being the first signs of block walls. It has been proposed that DRV characteristics be classed as creep, hot, warm, and cold DRV.[18,24–26]

IV. DYNAMIC RECRYSTALIZATION

In creep, a reduction in SFE decreases DRV and ε_s; it occasionally causes DRX in pure Cu and Ni,[66,67] but in hot working, it markedly changes behavior from that of Al or α Fe.[3–11,18,59–64,76,112,125–129] The discontinuous DRX mechanism is fairly common in hot working and is useful in lowering the flow stress (Figure 1(b) and raising the ductility, as explained in Section V; however, in many industrial situations, the strain is below the critical value of ε_{cDRX}. In creep, DRX is somewhat of a curiosity which is limited to pure metals; this is beneficial, since the spurts in $\dot{\varepsilon}$ and increased ε are not wanted.[66,67] As shown in Figure 5(b) ε_{cDRX}

declines with rising $\dot{\varepsilon}$ in the creep range and then rises in the hot-working range, as nucleation is impeded by the rapid reintroduction of substructure.[126–131] On the other hand, the critical strain for SRX (ε_{cSRX}) declines across the entire range. In the case of Ni at 1000 °C, ε_{cDRX} drops below ε_s over a broad range, but at 700 °C, the potential range is rather narrow and fracture usually precludes DRX.[61,126] As for Al 99.9 pct, ε_s is much below ε_{cDRX}, so classical DRX does not occur.[132] For Al 99.999 pct, the greatly augmented GB mobility markedly lowers ε_{cDRX} (and ε_{cSRX}), so that it becomes less than ε_s, which is reduced only a little.[77–80,132]

In contrast, for γ stainless steels, increased solute lowers both the SFE (raising θ and the possible ε_s level for DRV) and the GB mobility (raising ε_{cDRX}), leading to high σ_p and σ_s values.[59,62–64,76,128–130] Fine particles (carbides in austenite and γ' (Ni$_3$Al) in superalloys) raise ε_c and σ_p.[3–10,60,61] During the classical discontinuous form in Cu, Ni, and γ Fe, nucleation starts at σ_c (ε_c), as determined from θ-σ curves (Figure 5(a)) and as confirmed by microscopy; ε_c is about 0.7 ε_p (Figure 1(b)). Necklaces of new grains form along the GBs, progressively replacing the original grains.[126–132] The GBs are serrated, and nuclei seem to form by some of them becoming rotated to form a mobile GB at their neck with the parent grain. The grain size (D_s) is about 10 times that of subgrains and is dependent on T and $\dot{\varepsilon}$ with the same form as in Eqs. [5] and [6], but in the latter, D_s
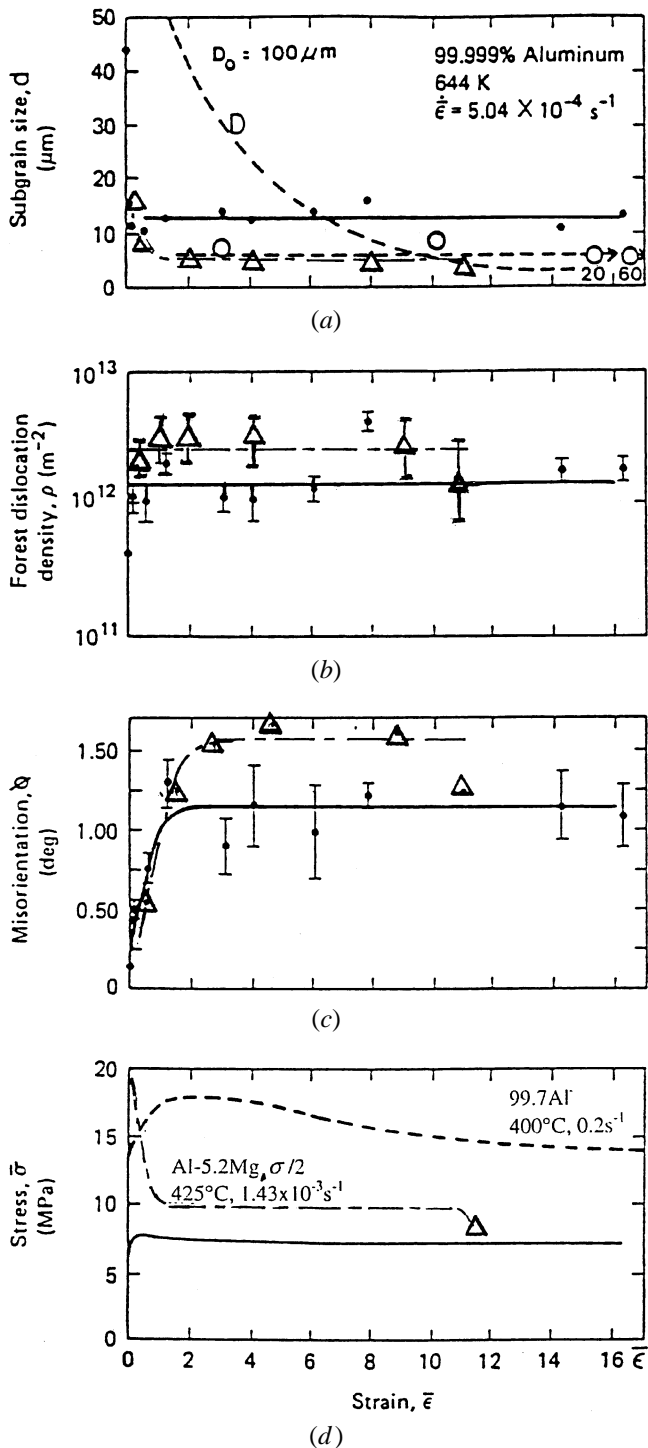
Fig. 9—The evolution of substructure in Al and Al-Mg at high strains: (a) subgrain sizes in comparison to grain size; (b) internal dislocation density; (c) misorientation; and (d) flow curves (Al-Mg σ/2, 99.7Al to ε = 60) (Al,[54] and McQueen and co-workers,[52,53] and Al-5.2Mg,[56]).

has a power near −1.25 (Figure 10(c)).[62–64,76] As D_s becomes larger relative to the original grain size (D_O), there are multiple discrete waves indicated by several peaks in the flow curve,[127] similar to the repeated excursions in creep. In single crystals, nucleation occurs at much larger strains than for necklace formation at GBs and is defined by a critical σ 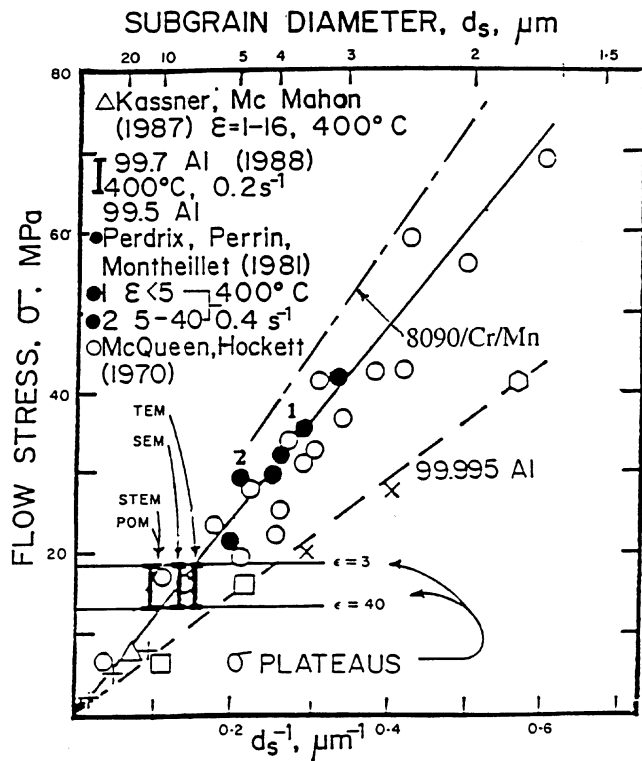level, which depends on T and $\dot{\varepsilon}$.[67] After the initiation of the first DRX grain and its growth by multiple twin formation, the stress falls to a value similar to polycrystals.[67,128,131]

In Al alloys, there are several forms of DRX, in addition to geometric DRX, that do not occur in Cu or Ni because of classical DRX at lower strains. At large hard particles (>1 μm), the additional compensating turbulent flow in the matrix produces smaller cells at 20 °C, which leads to particle-stimulated nucleation (PSN) in alloys such as Al-Mn and Al-Mg-Mn. At high T values, DRV in a simple Al matrix eliminates such cells but does not do so in Al-Mg alloys, where the level of DRV is reduced so that PSN-DRX nucleates at the particles[133] (also observed at segregated α particles in as-cast γ stainless steels).[62,79,80,90] Classical DRX is not found in Al-5Mg, apparently because ε_{cDRX} is raised more by the decrease in GB mobility than ε_s is raised by the pinning of dislocations; all reports of it appear to arise from geometric DRX.[27,57,72,94,95] Continuous DRX has been found in alloys such as Al-Cu-Zr (supral) and Al-10Mg-Zr (or -Cr, -Mn), which have been predeformed at a high Z level (~300 °C) after a suitable dispersion of pinning particles has been established by heat treatment.[14,15,79,80,134–136] Such DRX takes place upon straining at a low Z level (~10−3s1 and ~500 °C) in the initial stage of superplastic deformation. The high-ψ dislocation walls stretching between the pinning particles transform into grain boundaries, which are mobile (except for the particles) and capable of sliding to impart superplastic behavior. Continuous DRX has been postulated in Al, in the absence of pinning particles, as an explanation of the development of some high-ψ walls inside the grains (Figure 11(b)),[123,124] but this can be classified as warm DRV, as discussed earlier. Continuous DRX has also been applied to development during warm straining of high-ψ cells in either ferritic stainless steel or in austenitic stainless steel below the T value where classical DRX is observed.[26] The simple generation of high-misorientation cells, which occurs in cold working, is not considered to be recrystallization until new grains actually form in annealing.[26,121]
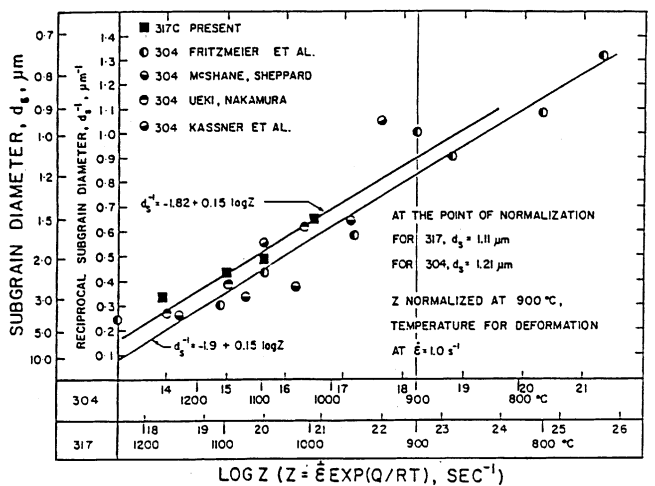
Dynamic grain growth with excursions of accelerated straining has been observed in large-grained Al as a result of sudden GB migrations across substantial volumes of the specimen eliminating the substructure.[137] There is no nucleation of new grains and a net enlargement of grain size. This can be considered as stress-induced boundary migration, but is over such long segments that nuclei do not form. Such boundary migrations of lesser extent repeatedly occur in most creep conditions and produce a net consumption of grains with a denser substructure and continual growth of the average grain size.[26,138–141] This is similar to the gradual elimination of grains with a higher dislocation density in geometric DRX, as explained earlier.[26,113]

V. ELEVATED-TEMPERATURE DUCTILITY

In contrast to creep, where a long service life and a low strain are ideal, in hot working, a high strain to rupture (ε_f) is a particularly valuable property. When fracture arising from casting segregation, voids, and inclusions is avoided, the basic mechanism is the linking together of fissures caused by the propagation of w-cracks which originate at triple junctions from grain-boundary sliding;[1,3,4,8,11,12,61,142,143,144] this occurs even though sliding is only 1 to 2 pct of the strain compared to 5 to 30 pct in creep, as $\dot{\varepsilon}$ falls.[30,32,144]

SUBGRAIN DIAMETER, d_s, μm

$\triangle$ Kassner, Mc Mahon
(1987) $\dot{\varepsilon}$=1-16, 400°C

I 99.7 Al (1988)
400°C, 0.2 s^{-1}
99.5 Al

● Perdrix, Perrin,
Montheillet (1981)

◑ 1 $\dot{\varepsilon}$ <5 ⌐ 400°C
● 2 5-40 ⌐ 0.4 s^{-1}

○ McQueen, Hockett
(1970)

TEM
SEM
STEM
POM

8090/Cr/Mn

99.995 Al

$\varepsilon = 3$
$\varepsilon = 40$

σ PLATEAUS

FLOW STRESS, σ, MPa

d_s^{-1}, μm^{-1}

(*a*)

■ 317C PRESENT
○ 304 FRITZMEIER ET AL.
◕ 304 McSHANE, SHEPPARD
◓ 304 UEKI, NAKAMURA
◑ 304 KASSNER ET AL.

SUBGRAIN DIAMETER, d_s, μm

RECIPROCAL SUBGRAIN DIAMETER, d_s^{-1}, μm^{-1}

d_s^{-1} = -1.82 + 0.15 log Z

d_s^{-1} = -1.9 + 0.15 log Z

AT THE POINT OF NORMALIZATION
FOR 317, d_s = 1.11 μm
FOR 304, d_s = 1.21 μm

Z NORMALIZED AT 900 °C,
TEMPERATURE FOR DEFORMATION
AT $\dot{\varepsilon}$ = 1.0 s^{-1}

| 304 | 14 1200 | 15 1100 | 16 1000 | 17 | 18 900 | 19 | 20 800 °C | 21 |

| 317 | 18 1200 | 19 1100 | 20 | 21 1000 | 22 | 23 900 | 24 | 25 800 °C | 26 |

LOG Z (Z = $\dot{\varepsilon}$ EXP(Q/RT), SEC^{-1})

(*b*)

GRAIN AND SUBGRAIN SIZE, μm

D_u

◇ 301W 66 Ryan, McQueen
◗ 304W 220 Ahlblom
◔ 304W 250 Barraclough
◑ 304W 150 Maki et al
○ 304W 70
△ 316W 63 Ryan, McQueen
■ 317W 72
□ 317W 57
⊡ 317W 75 Boden

MRX $\sigma_s = 8.8 D_{MRX}^{-0.76}$

DRX $\sigma_s = 4.7 D_s^{-0.81}$

SUBGRAIN SIZE, Al ALLOYS

SUBGRAIN SIZE
AUSTENITIC STAINLESS

STEADY STATE FLOW STRESS, σ_s (MPa)

(*c*)

Fig. 10—Subgrain sizes related to deformation conditions: (*a*) to σ for Al with ε near 3 and for ε from 5 to 40, the stress varies due to Taylor softening from a plateau near 3 to another near 40[52,53] (with comparison to 8090/Cr/Mn (Fig. 6)[53,170]); (*b*) to $\dot{\varepsilon}$ and T through Z for 304 and 317C; and (*c*) to σ for 300 series steels with comparison to Al and to dynamically recrystallized grains.[18,62–64,76]

The cause of very good ductility (Figure 12(a)) rising with temperature in high-recovery metals (Al, α Fe, Fe-Cr, Fe-Si) is the virtual elimination of crack formation by the ability of the lattice to accommodate sliding near triple points and by the reduction in sliding itself due to serrations of the boundaries from interactions with sub-boundaries.[12,52–55,142,143] At much higher T levels, ductility declines because of increasing r-pore formation at GBs due to vacancy migration.[145,146] The results of Myshlyaev and co-workers[55,114] confirm the high ductility, although their T dependence seems unsatisfactory.[145] Such ultraductility is related to

DRV and geometric DRX[52–55] and not to fine-grained superplasticity,[55,79,114] since a strong texture becomes stable.[53,54,113]

In low-recovery metals, the accommodation and serrations are insufficient to avoid cracking and the ductility drops as T rises near 0.5 to 0.6 T_m.[147,148] At higher temperatures, ε_f rises markedly as dynamic recrystallization relieves the stress concentrations and moves the boundaries away from any cracks (Figures 1(b) and 12(b)).[3,8,11,60–63,142,143,147,148] The multistage schedules in rolling and forging raise ductility when recrystalization between stages fills the same role as
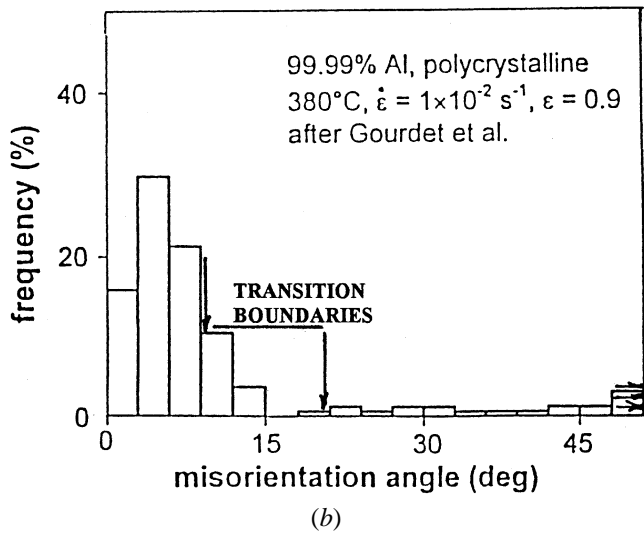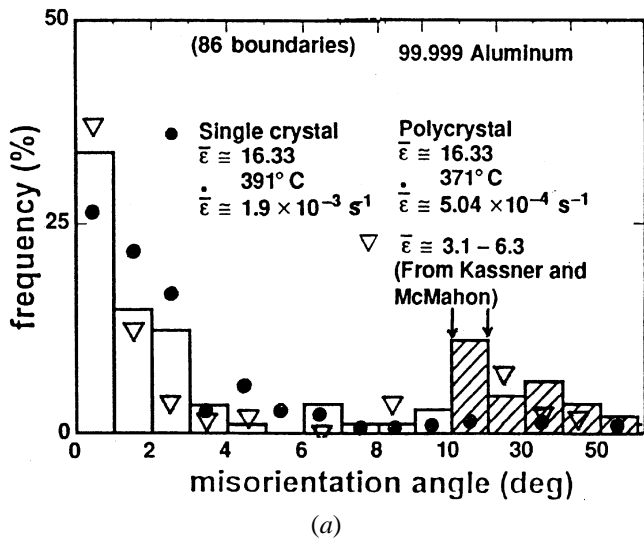
Fig. 11—Distributions of misorientations in Al at various strains: (a) poly-crystal at $\varepsilon = 4$ and with single crystal at $\varepsilon = 16.33$ by TEM; and (b) polycrystals at $\varepsilon = 0.9$ from Kikuchi analysis in SEM-EBS. The transition boundary range is marked by vertical arrows and the ψ of each TB increases as ε rises.[24,25,26] (a) Ref. 54 and (b) Ref. 123.

DRX. The isolated cracks tend to spheroidize and can only extend when they snare a migrating boundary. Because of the accumulations of pores, the ductility is only one-fifth that of high-recovery metals. As an example, in comparison to Fe-25Cr with $\varepsilon_f > 100$, the torsion ductility of homogenized 317 steel (37 pct Cr + Ni + Mo) is ~10, but for the as-cast alloy with about 20 pct segregated α particles, it is only 1.2, due to interphase cracking.[62,142,149] Constitutive equations somewhat similar to those in creep have been developed to predict ε_f in homogeneous alloys.[8,63,76]

In hot shaping, good inherent ductility provides for easy breakdown of the as-cast structure, a high strain per pass for greater production rates, the avoidance of surface cracks which require expensive removal, a lower scrap rate, the omission of non-destructive testing for many products, or an optimum combination of these.[142] In addition, the ductility is required over a temperature range to allow for cooling from the preheat temperature due to radiation during part
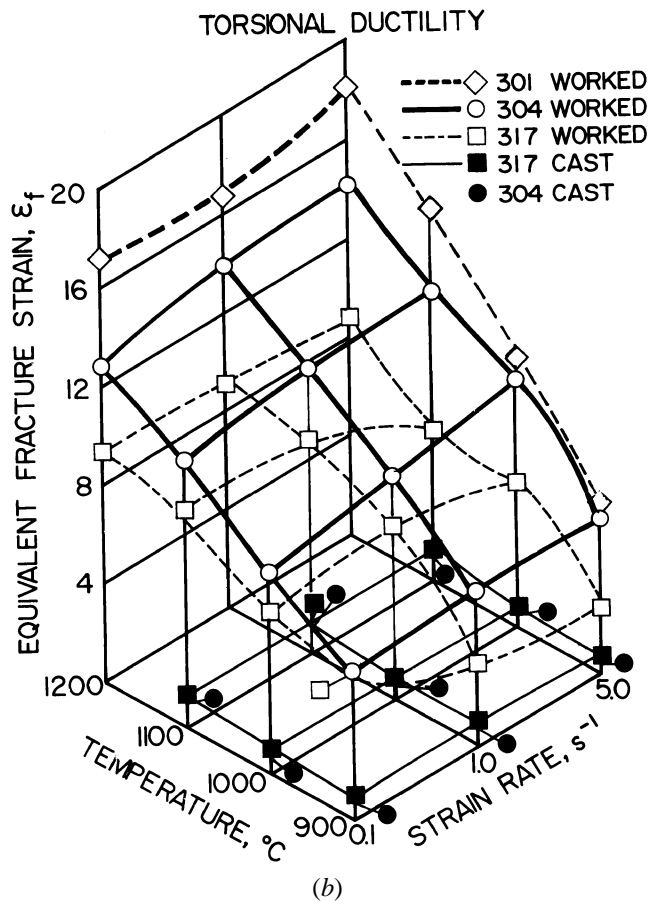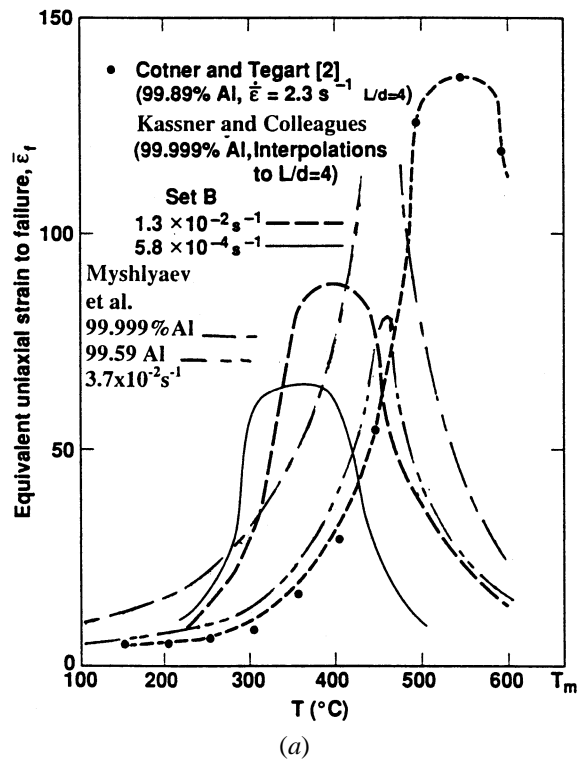

Fig. 12—Ductility in torsion of (a) Al with peaks in the range 350 °C to 550 °C 2 to 0.001 s^{-1}.[55,114,145] and (b) of 304W and 317W in comparison to 317C and 304C, low due to cracking at ferrite austenite interfaces. (a) Ref. 145 and (b) Refs. 62 through 64 and 76.

manipulation and conduction to cold tooling. Pure high-recovery metals generally have a range well in excess of requirements; however, their alloys suffer a somewhat narrowed range because of the lowered solidus temperature and a more rapid decline in ductility with temperature decrease, as the ability to accommodate sliding is curtailed by raised lattice strength.[8,143] While for low-SFE metals the range is usually adequate despite the minimum in ductility below the dynamic recrystallization temperature,[147,148] alloys of these metals often present great difficulty, because the DRX temperature is so close to the solidus temperature as a result of solute segregation and particles inhibiting boundary migration.[60,143,149] Some Ni superalloys are so heavily alloyed for creep resistance that their potential working range above the γ' solvus is too narrow for processing to be feasible; however, in powder-metallurgy material, fine grains and limited segregation facilitates forging. In most working operations, the presence of a mean compressive stress is beneficial in healing w-cracks and even casting defects (if unoxidized).[142,143] However, regions with tensile components can be induced by tooling configuration, friction, and cooling.[142] Because of differences in the mean stress, the hot workability from laboratory tests must be empirically scaled against specific processes.[2]

Failure-mechanism maps have been extensively developed for creep in relation to quantified facture mechanisms. In some cases, hot-working results have been added with a region at high T and $\dot{\varepsilon}$, which is labeled DRX, giving the impression that it is a failure mode.[146] As just explained, DRX retards GB fissuring and leads toward a fracture mode called rupture, with very high reductions in area. Empirical fracture maps have been developed for specific alloys based on specific microstructures and modes of cracking; these can be valuable guides.[146] Maps of energy-dissipation efficiency, related to strain-rate sensitivity through a special theory, have been used to predict domains of DRX and of instability.[58,59,132] The imputation of DRX to Al is in contradiction to extensive evidence;[58] the predictions of the high ε_f values of stainless steels following long steady-state regimes are highly inaccurate, since they are based only on the peak and work softening.[58,132]

VI. DYNAMIC PRECIPITATION AND COALESCENCE

In creep service, alloys are usually heat treated to an optimum condition of precipitation to provide prolonged resistance to extension. During the long creep service, there would be coalescence of the particles;[38–40,150] in Ni-based superalloys, there is rafting of the γ', which facilitates dislocation passage through the matrix. This is a problem even in rapidly solidified alloys selected for the stability of their particles and for the low solubility and diffusion rates of their elements. In hot working of Ni-based alloys, working usually starts above the solvus and precipitates form during the cooling, causing a rise in the flow stress and a drop in ductility;[60] in torsion testing, coalescence of γ' has been observed with marked flow softening and high ductility.[151,152] In overheating such alloys, the carbides dissolve and may reprecipitate at the grain boundaries, enhancing GB cracking. In TMP of these alloys, there are several stages

at selected reducing temperatures of precipitation to provide pinning particles for the following deformation.[153]

In steels, it is common to preheat the austenite to dissolve all particles and, thus, control their size and distribution subsequently. This is of great consequence in microalloyed steels; Nb(CN) undergoes enhanced dynamic precipitation (DPN) during the final rolling stages to inhibit SRX of the austenite.[6,10,17,154,155] In hypereutectoid steels, working the austenite is easy except where alloy carbides remain undissolved.[71] In the intercritical region, the layer of carbide, if allowed to grow, can cause GB cracking. However, continual working during the cooling causes the carbide particles to deform and separate into small particles which lead to material with good superplasticity, notably in the ferritic condition.[156] In ferritic steels, the increase in pearlite fraction with rising C content raises the flow stress and reduces the usually exceptional ductility; spheroidite is much softer and more ductile.[156] Working close to the eutectoid T level causes very rapid spheroidization of the pearlite with flow softening and attainment of very high ductility.[156] Heavy hot deformation (98 pct reduction) of an Al-0.65 Fe conductor rod extends the eutectic colonies (Al₃Fe rods 5-μm long) around 20 μm dendrites into long stringers closely spaced, so that the divided particles (0.5 μm in length) have a spacing of 2.5 μm.[98,157]

In Al alloys, preheating for rolling dissolves the age-hardening elements which precipitate between stages principally as equilibrium particles which cause little strengthening; however, preheating below the solvus can produce large GB precipitates and low ductility, notably in 7000-series alloys.[158] If alloys are rapidly cooled from homogenization soaking for extrusion near 300 °C, then DPN in early straining leads to retardation of DRV and high peak flow stresses, which severely raises the initial breakthrough pressure (Figure 13).[42,158,159] Pretreatment to medium particles overcomes this difficulty and avoids surface defects; furthermore, such particles dissolve in the extrusion hot zone ($\Delta T \sim 50$ to 100 °C) just before the die, so that the emerging extrusion may be rapidly cooled in readiness for subsequent aging.[42,159]

VII. STATIC RECOVERY AND RECRYSTALLIZATION

Compared to cold working, the dislocation density in creep is very low, so that SRX is very unlikely. Static recovery (SRV) occurs, leading first to the loss and rearrangement of the dislocations in the subgrain interiors and in the walls and then, after much longer times, to growth of the subgrains.[160,161] Creep service is usually very lengthy, but there are periods of load removal while remaining at high T levels; the loss of dislocations by SRV results in enhanced creep on reloading, but the transient is shorter than on initial loading. After hot working, recovery proceeds more rapidly than after creep and usually proceeds to a greater extent than after cold working, because of the delay in SRX nucleation due to the less-dense substructure.[4,9,12,72] In general, the time for SRX and the grain size can be decreased by raising the strain (accumulated since the previous SRX, but only up to ε_s) and strain rate and lowering the deformation temperature.[12,72,121] In Al and α Fe, SRX tends to be very slow but may be altered by alloying, such as retarding by fine
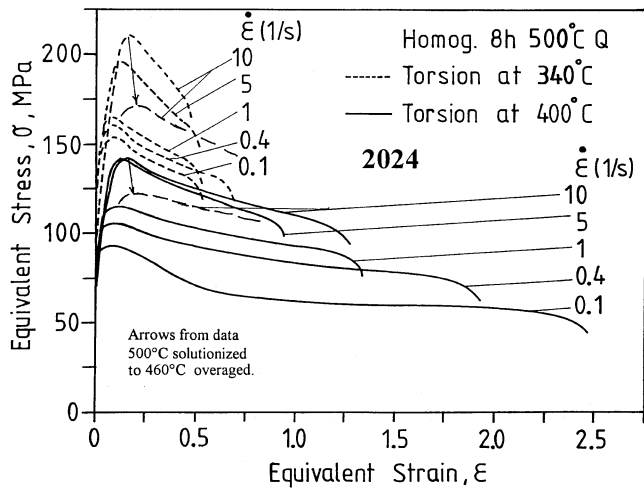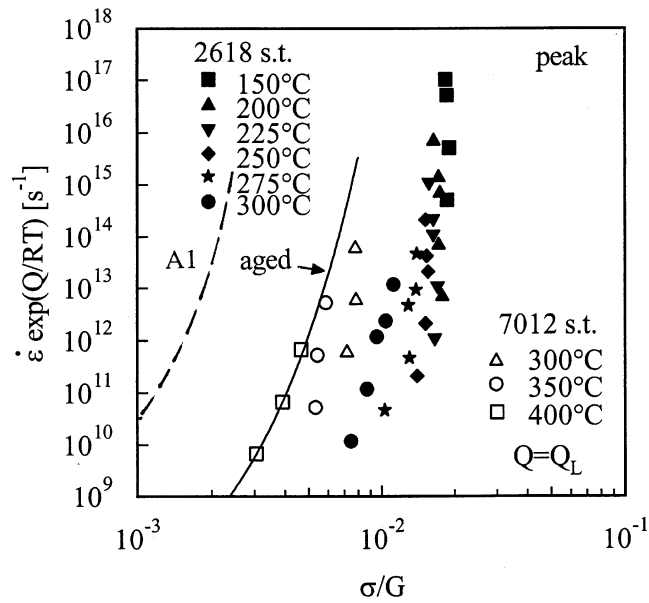
Fig. 13—Dynamic precipitation[159] is illustrated for (a) 2024 alloy in flow curves after solution at 500 °C with sharper peaks from finer particles at 340 °C than at 400 °C (peaks for partial aging at 460 °C are much lower, as indicated by vertical arrows to 10 s⁻¹ curves) and (b) by peak stresses in 7012 (≥300 °C) and 2618 (≤300 °C, larger effect) both aged (almost similar along line) and solution treated (st) for various $\dot{\varepsilon}$ and T normalized, as in Fig 4. (a) Ref. 172 and (b) Ref. 173.

(<0.5 μm) dispersoids[98,157] and precipitates in age-hardenable Al alloys or accelerating by Mg solute or large dispersoids (>2 μm).[44,90,133] In low-SFE metals such as Cu, Ni, and γ Fe, SRX tends to be very fast because of the much denser substructure; alloying with solute such as in austenitic stainless steel (~30 wt pct) slows SRX.[4,6,10,17,61,162,163] After the initial high-temperature stages of rolling schedules, SRX is generally expected in the intervals and is an important objective in grain refinement,[6,9,10,17,162–164] but is sometimes difficult in Al and α Fe alloys. If no SRX takes place, a strong texture develops (in Al, 45-deg ears in cup drawing) and, after that, holding or final annealing produces a strong SRX texture (in Al, a cube texture with 0- to 90-deg ears).[15,44,165] With SRX at several intermediate points, it is possible to produce a sheet with nearly planar isotropy.

VIII. THERMOMECHANICAL PROCESSING

While creep components may have been improved by TMP,[151–153] it is not likely that the creep service would be manipulated to provide a material with improved properties. In contrast, it is very common to design hot-working processes to improve properties; while saving total process steps (labor, time, and energy), it requires that the shape and derived properties be attained simultaneously (a final heat treatment after all shaping is simpler). The hot working and cooling can be arranged so that the metal is recrystallized to a suitable grain size and texture (as detailed in Section VII), usually in preparation for cold forming.[12,44,45,72] The alternative is to manipulate the deformation stages and final cooling to retain the final substructure.[14,16,93] In controlled rolling of high-strength low-alloy steels, NbCN particles help retain pancaked austenite, in which the substructure accelerates the transformation to very fine ferrite.[6,9,10,17,154,155,166–169] However, in C steels, the final stages and short intervals in a continuous mill (four to eight rolling stands) at a very low temperature postpone SRX until the end, so that the fine γ grains transform on rapid cooling to equally fine ferrite. The fine grain size provides a very low transition temperature and high yield strength augmented by fine microalloy carbonitrides.

There are many other cases where retention of the hot work substructure provides improved mechanical properties sometimes in conjunction with other strengthening mechanisms. In production of Al-Fe or Al-Fe-Co electrical wire, the wheel cast bar (6 × 9 cm²) is rolled in 13 passes[157] to 9.3mm diameter rod with about 1 μm subgrains; without recrystallizing, it is drawn (ε = 2.56) to 2.6mm wire with cells of 0.5 μm. The wire is recovery annealed (1.4 μm) to raise ductility from 4 to 30% suitable for bending during installation, while retaining excellent strength and thermal stability at 300°C (Table I).[12,14,15,98,157] With moderate cooling of Al alloys, extrusions retain a substructure increasing in density with radius and a duplex ⟨111⟩ and ⟨110⟩ texture which contributes about 20% increase in longitudinal strength; removal of a thick surface layer would cause serious weakening.[15,165] In 6000 series alloys, passage through the hot zone can be organized to serve as solution treatment so that rapid cooling at the die exit can be followed by straightening and aging.[15,49,159] Solution treatment of 2000 and 7000 series alloys to permit complex aging for balanced aircraft properties results in SRX with loss of texture and substructure strengthening. In steels, hot working of austenite and transformation to bainite carries over the dislocations to improve the structure; similarly warm working of austenite cooled below the pearlite nose causes the substructure to be carried into the martensite with considerable improvement in fatigue resistance (ausforming).[169]

IX. CONCLUSIONS

Creep and hot working share similar relationships of temperature, strain rate and stress with similar activation energies in cases where dynamic recovery is the principal

mechanism. In the hot working of low stacking fault energy metals, dynamic recrystallization is important in reducing the flow stress with increased activation energy and in improving ductility. In hot forming, cracking from limited grain boundary sliding is the fundamental fracture mechanism; however, inclusions or casting defects often curtail the ductility. In contrast to creep, the ideal material for hot working has low flow stress, high ductility and final microstructure tailorable to planned use.

Creep is able to provide detailed evidence on the gradual evolution of microstructure into the steady-state regime, which is cut short by failure mechanisms. Hot working, notably in torsion, is able to provide the evolution during the steady state up to a very mature stage where the grains have undergone severe elongation. Additionally, in hot working, DRX kinetics and microstructures have been determined. In the industrial domain, carefully processed creep-resistant alloys undergo slow coalescence of strengthening particles and development of voids. Hot forming often begins with as-cast segregated microstructures, but may incorporate additional manipulations of secondary phases to thermomechanically produce improved materials. While there is a slow transfer of fundamental knowledge, creep engineers and metal workers communicate directly only about creep-resistant alloys.

REFERENCES

1. E.E. White and C. Rossard: *Deformation Under Hot-Working Conditions*, Iron and Steel Institute, London, 1968, pp. 14-20.
2. H.J. McQueen and J.J. Jonas: *Metal Forming: Interrelation between Theory and Practice*, Plenum Press, New York, NY, 1971, pp. 393–429.
3. C.M. Sellars and W.J.McG. Tegart: *Int. Met. Rev.*, 1972, vol. 17, pp. 1-24.
4. H.J. McQueen and J.J. Jonas: *Treatise on Materials Science and Technology, Plastic Deformation of Materials*, Academic Press, New York, 1975, vol. 6, pp. 343-93.
5. H. Mecking and G. Gottstein: *Recrystallization of Metallic Materials*, Dr. Riederer Verlag, Stuttgart, 1977, pp. 195-222.
6. C.M. Sellars: *Hot Working and Forming Processes*, The Metals Society, London, 1980, pp. 3-15.
7. H.J. McQueen: *Met. Forum (Australia)*, 1981, vol. 4, pp. 81-91.
8. A. Gittins and W.J.McG. Tegart: *Met. Forum*, 1981, vol. 4, pp. 57-62.
9. H.J. McQueen and J.J. Jonas: *J. Appl. Met. Working*, 1984, vol. 3, pp. 233-41 and 410-20.
10. W. Roberts: *Strength of Metals and Alloys*, ICSMA 7, H.J. McQueen *et al.*, eds., Pergamon Press, Oxford, United Kingdom, 1986, pp. 1859-92.
11. H.J. McQueen and D.L. Bourell: *J. Met.*, 1987, vol. 39 (7), pp. 28-35.
12. H.J. McQueen: *Hot Deformation of Aluminum Alloys*, T.G. Langdon and H.D. Merchant, eds., TMS-AIME, Warrendale, PA, 1991, pp. 31-54.
13. H.J. McQueen: *Asia Pacific Conf. Materials Proc.*, Singapore, 1993, *J. Mater. Proc. Technol.*, 1993, vol. 37, pp. 3-36.
14. H.J. McQueen and J.J. Jonas: *Aluminum Alloys '90*, 2nd Int. Conf., Beijing, C.Q. Chen and E.A. Starke, eds., International Academic Publishers, Beijing, 1990, pp. 727-42.
15. H.J. McQueen and M.E. Kassner: *Lightweight Alloys for Aerospace Applications*, K. Jata, ed., TMS-AIME, Warrendale, PA, 2001, in press.
16. H.J. McQueen, E. Evangelista, and N.D. Ryan: *Processes & Materials Innovation, Stainless Steel 1993*, Florence, W. Nicodemi, ed., Associazione Italiana di Metallurgia, Milan, 1993, vol. 2, pp. 289-302.
17. H.J. McQueen, S. Yue, N.D. Ryan, and E. Fry: in *Advanced Materials and Technologies*, L.A. Dobrzanski, ed., Silesian Technical University, Gliwice, Poland, 1995, pp. 295-332.
18. H.J. McQueen: *Jonas Symp. on Thermomechanical Processing, Texture and Formability of Steel*, E. Essadiqi and S. Yue, eds., TMS-CIM, Montreal, 2000, pp. 323-33.
19. H.J. McQueen and H. Mecking: *Creep and Fracture of Engineering Materials and Structures*, Pineridge Press, Swansea, United Kingdom, 1984, pp. 169-84.
20. H.J. McQueen, W. Blum, Q. Zhu, and V. Demuth: in *Advances in Hot Deformation Textures and Microstructures*, J.J. Jonas, T.R. Bieler, and K.J. Bowman, eds., TMS-AIME, Warrendale, PA, 1993, pp. 235-50.
21. W. Blum and H.J. McQueen: in *Aluminum Alloys, Physical and Mechanical Properties*, (ICAA5), J.H. Driver, B. Dubost, F. Durand, R. Fougeres, P. Guyot, P. Sainfort, and M. Suery, eds. *Mater. Sci. Forum*, 1996, vols. 217–222, pp. 31-42.
22. Q. Zhu, W. Blum, and H.J. McQueen: *Aluminum Alloys, Physical and Mechanical Properties*, ICAA5, Grenoble, J.H. Driver, B. Dubost, F. Durand, R. Fougeres, P. Guyot, P. Sainfort, and M. Suery, eds., Trans Tech Pub., Aedermannsdorf, Switzerland; *Mater. Sci. Forum*, 1996, vols. 217–222, pp. 1169-74.
23. W. Blum, Q. Zhu, R. Merkel, and H.J. McQueen: *Al Alloys, Physical Mechanical Properties*, ICAA5, J.H. Driver, B. Dubost, F. Durand, R. Fougeres, P. Guyot, P. Sainfort, and M. Suery, eds., Trans Tech Pub., Aedermannsdorf, Switzerland. *Mater. Sci. Forum*, 1996, vols. 217–222, pp. 611-16.
24. H.J. McQueen and W. Blum: *Recrystallization and Related Topics.* Rex '96, T.R. McNelley, ed., Monterey Institute of Advanced Studies, Monterey, CA, 1997, pp. 123-36.
25. H.J. McQueen and W. Blum: *Al Alloy Physical and Mechanical Properties, ICAA6*, T. Sato, ed., Japan Institute of Metals, 1998, pp. 99-112.
26. H.J. McQueen and W. Blum: *Mater. Sci. Eng.*, 2000, vol. A290, pp. 95-107.
27. W. Blum, Q. Zhu, R. Merkel, and H.J. McQueen: *Z. Metalkd*, 1996, vol. 87, pp. 341-48.
28. W. Blum, Q. Zhu, R. Merkel, and H.J. McQueen: *Mater. Sci. Eng.*, 1996, vol. A205, pp. 23-30.
29. J.E. Dorn: *Creep and Recovery*, ASM, Metals Park, OH, 1957, pp. 255-83.
30. J. Weertman: *J. Appl. Phys.*, 1957, vol. 28, pp. 362-64.
31. F. Garofalo: *Fundamentals of Creep, Creep Rupture in Metals*, Macmillan, New York, 1965.
32. H. Conrad: *Mechanical Behavior of Materials at High Temperature*, J.E. Dorn, ed., McGraw-Hill, New York, NY, 1961, pp. 149-217.
33. W.D. Nix and B. Ilschner: *Strength of Metals and Alloys*, ICSMA 5, P. Haasen, V. Gerold, and G. Kostorz, eds., Pergamon Press, Oxford, United Kingdom, 1979, pp. 1503-30.
34. A.K. Mukherjee: *Treatise on Materials Science and Technology*, vol. 6, *Plastic Deformation of Materials*, Academic Press, New York, NY, 1975, pp. 164-225.
35. H. Oikawa and T.G. Langdon: *Creep Behaviour of Crystalline Solids*, B. Wilshire and R.W. Evans, eds., Pineridge Press, Swansea, United Kingdom, 1985, pp. 33-82.
36. J.L. Martin: in *Creep Behaviour of Crystalline Solids*, B. Wilshire and R.W. Evans, eds., Pineridge Press, Swansea, United Kingdom, 1985, pp. 1-32.
37. M.E. Kassner and M.-T. Perez-Prado: *Progr. Mater Sci.*, 2000, vol. 45, pp. 1-102.
38. W. Blum: *Plastic Deformation and Fracture of Materials*, H. Mughrabi, ed., VCH, Weinheim, 1993, pp. 359-405.
39. M.E. Kassner, J.W. Elmer, and C.J. Echer: *Metall. Trans. A*, 1986, vol. 17A, pp. 2093-97.
40. S. Straub and W. Blum: in *Hot Workability of Steels and Light Alloys-Composites*, H.J. McQueen, E.V. Konopleva, and N.D. Ryan, eds., TMS-CIM, Montreal, 1996, pp. 189-204.
41. H.J. McQueen and O.C. Celliers: *Mater. Forum (Australia)*, 1993, vol. 17, pp. 1-13.
42. H.J. McQueen and O.C. Celliers: *Can. Metall. Q.*, 1997, vol. 36, pp. 73-86.
43. M. Sauerborn and H.J. McQueen: *Mater. Sci. Technol.*, 1998, vol. 14, pp. 1029-38.
44. H.J. McQueen: *JOM*, TMS, Warrendale, PA, 1998, vol. 50 (6), pp. 28-33.
45. I. Poschmann and H.J. McQueen, *Z. Metallkd.*, 1997, vol. 88, pp. 14-22.
46. E. Evangelista, N.D. Ryan, and H.J. McQueen: *Metall. Sci. Technol.*, 1991, vol. 9, pp. 75-92.
47. N.D. Ryan and H.J. McQueen: *J. Mech. Working Tech.*, 1986, vol. 12, pp. 279-96 and 323-49.
48. W. Blum, P. Weidinger, B. Watzinger, R. Sedlacek, R. Rosch, and H.G. Haldenwanger: *Z. Metallkd.*, 1977, vol. 88, pp. 636-41.
49. W. Blum, P. Zhang, B. Watzinger, B.V. Grossman, and H.G. Haldenwanger: ICSMA 12, M. Mills, ed., *Mater. Sci. Eng. A*, 2000, in press.

50. K.P. Rao, E.B. Hawbolt, H.J. McQueen, and D. Baragar: *Can. Metall. Q.*, 1993, vol. 32, pp. 165-75.
51. H.J. McQueen and J.E. Hockett: *Metall. Trans.*, 1970, vol. 1, pp. 2997-3004.
52. O. Knustad, H.J. McQueen, N. Ryum, and J.K. Solberg: *Practical Metall.*, 1985, vol. 22, pp. 215-29.
53. J.K. Solberg, H.J. McQueen, N. Ryum, and E. Nes: *Phil. Mag.*, 1989, vol. 60, pp. 447-71 and 473-85.
54. M.E. Kassner and M.E. McMahon: *Metall. Trans. A*, 1987, vol. 18A, pp. 835-46.
55. M.E. Kassner, M.M. Myshlyaey, and H.J. McQueen: *Mater. Sci. Eng.*, 1989, vol. A108, pp. 45-61.
56. G.A. Henshall, M.E. Kassner, and H.J. McQueen: *Metall. Trans. A*, 1992, vol. 23A, pp. 881-89.
57. H.J. McQueen, J. Belling, and E. Fry: *J. Eng. Mater. Performance*, 2001, vol. 10, pp. 164-72.
58. H.J. McQueen, E. Evangelista, N. Jin, and M.E. Kassner: *Metall. Trans. A*, 1995, vol. 26A, pp. 1757-66.
59. H.J. McQueen, N. Jin, and N.D. Ryan: *Mater. Sci. Eng*, 1995, vol. A190, pp. 43-53.
60. H.J. McQueen, G. Gurewitz, and S. Fulop: *High Temp. Technol.*, 1983, vol. 2, pp. 131-38.
61. M.J. Luton and C.M. Sellars *Acta Met.*, 1969, vol. 17, pp. 1033-43.
62. E. Evangelista, N.D. Ryan, and H.J. McQueen: *Met. Sci. Technol.*, 1987, vol. 5 (2), pp. 50-58.
63. N.D. Ryan and H.J. McQueen: *J. Mater. Proc. Technol.*, 1990, vol. 21, pp. 177-99.
64. N.D. Ryan and H.J. McQueen: *High Temp. Technol.*, 1990, vol. 8, pp. 185-200.
65. J. Hausselt and W. Blum: *Acta Metall.*, 1976, vol. 14, pp. 1027-39.
66. G.J. Richardson, C.M. Sellars, and W.J.McG. Tegart: *Acta Metall.*, 1966, vol. 14, pp. 1225-36.
67. G. Gottstein: *Met. Sci.*, 1983, vol. 17, pp. 497-502.
68. H.J. McQueen and N.D. Ryan: *Rate Processes in Plastic Deformation II*, S.V. Raj *et al.*, eds., TMS-AIME, Warrendale, PA, 2001, in press.
69. N.D. Ryan and H.J. McQueen: *Stainless Steels '87*, Institute of Metals, London, 1988, pp. 498-507.
70. W.A. Wong and J.J. Jonas: *Trans TMS-AIME*, 1968, vol. 242, pp. 2271-80.
71. C.A.C. Imbert and H.J. McQueen: *Mat. Sci. Eng.,* 2001, vol. A313, pp. 88-103 and 104-116.
72. H.J. McQueen and N. Ryum: *Scand. J. Met.*, 1985, vol. 14, pp. 183-94.
73. H. Mecking: *Dislocation Modelling of Physical Systems*, M.F. Ashby *et al.*, Pergamon Press, Oxford, United Kingdom, 1980, pp. 197-211.
74. B. Nicklas and H. Mecking: in *Strength of Metals and Alloys*, P. Haasen, V. Gerold, and G. Kostorz, eds., Pergamon Press, Oxford, United Kingdom, 1979, vol. 1, pp. 351-56.
75. U.F. Kocks: *J. Eng. Mater. Technol., (ASME H)*, 1976, vol. 98, pp. 76-85.
76. N.D. Ryan and H.J. McQueen: *High Temp. Technol.*, 1990, vol. 8, pp. 27-44.
77. M.E. Kassner, H.J. McQueen, J. Pollard, E. Evangelista, and E. Cerri: *Scripta Metall. Mater.*, 1994, vol. 31, pp. 1331-36.
78. H. Yamagata: *Scripta Metall. Mater.*, 1994, vol. 30, pp. 411-16.
79. H.J. McQueen, E. Evangelista, and M.E. Kassner: *Z. Metallkd.*, 1991, vol. 82, pp. 336-45.
80. H.J. McQueen: *Light Metals 2000*, J. Kasudi and J. Masuunave, eds., TMS-CIM, Montreal, 2000, pp. 287-96.
81. R. Lombry, C. Rossard, and B.J. Thomas: *Rev. Met. CIT*, 1981, vol. 78, pp. 975-88.
82. J-P.A. Immarigeon and J.J. Jonas: *Acta Metall.*, 1971, vol. 19, pp. 1053-61.
83. H.J. McQueen, W.A. Wong, and J.J. Jonas: *Can. J. Phys.*, 1967, vol. 45, pp. 1225-34.
84. V.K. Lindroos and H.M. Miekkoja: *Phil. Mag.*, 1967, vol. 16, pp. 593-610; 1968, vol. 17, pp. 119-33.
85. S.F. Exell and D.M. Warrington: *Phil. Mag.*, 1972, vol. 26, pp. 1121-36.
86. D. Caillard and J.L. Martin: *Rev. Phys. Appl.*, 1987, vol. 22, pp. 169-83.
87. E.V. Konopleva, H.J. McQueen, and E. Evangelista: *Mater. Characterization*, 1995, vol. 34, pp. 341-48.
88. H.J. McQueen, N.D. Ryan, E.V. Konopleva, and X. Xia: *Can. Metal. Q.*, 1995, vol. 34, pp. 219-29.
89. M.R. Drury and F.J. Humphreys: *Acta Metall.*, 1986, vol. 34, pp. 2259-71.
90. E. Evangelista, H.J. McQueen, and E. Bonetti: *Deformation of Multiphase and Particle Containing Materials*, Risø National Laboratory, Roskilde, Denmark, 1983, pp. 243-50.
91. L. Fritzmeier, M. Luton, and H.J. McQueen: in *Strength of Metals and Alloys*, P. Haasen, V. Gerold, and G. Kostorz, eds., Pergamon Press, Oxford, United Kingdom, 1979, vol. 1, pp. 95-100.
92. S.V. Raj and G.M. Phari: *Mater. Sci. Eng.*, 1986, vol. 81, pp. 217-37.
93. D.J. Abson and J.J. Jonas: *Met. Sci.*, 1970, vol. 4, pp. 24-28.
94. T. Sheppard, M.G. Tutcher, and H.M. Flower: *Met. Sci.*, 1979, vol. 13, pp. 473-81.
95. E. Cerri, E. Evangelista, and H.J. McQueen: *High Temp. Mater. Proc.*, 1999, vol. 18, pp. 227-40.
96. I. Poschmann and H.J. McQueen: *Scripta Metal. Mater.*, 1996, vol. 35, pp. 1123-28.
97. K.G. Gardiner and R. Grimes: *Met. Sci.*, 1979, vol. 13, pp. 216-22.
98. H.J. McQueen, G. Avramovic-Cingara, and K. Conrod: *Can. Metall. Q.*, 1993, vol. 32, pp. 375-86.
99. H.J. McQueen and E.V. Konopleva: *Adv. Ind. Mater.*, Calgary, 1998, D.S. Wilkinson, W.J. Poole, and A. Alpas, eds., TMS-CIM, Montreal, 1998, pp. 149-60.
100. M.M. Myshlyaev, H.J. McQueen, A. Mwembela, and E.V. Konopleva: *Mater. Sci. Eng.*, 2001, in press.
101. J.A. Saeter and E. Nes: *Mater. Sci. Forum*, 1996, vols. 217–222, pp. 447-52.
102. M. Hatherley: *Strength of Metals and Alloys*, ICSMA6, R.C. Gifkins, ed., Pergamon Press, Oxford, United Kingdom, 1982, vol. 3, pp. 1181-95.
103. B. Bay, N. Hansen, D.A. Hughes, and D. Kuhlmann-Wilsdorf: *Acta Metall. Mater.*, 1992, vol. 40, pp. 205-19.
104. D.A. Hughes and N. Hansen: in *Advances in Hot Deformation Textures and Microstructures*, J.J. Jonas, T.R. Bieler, and K.J. Bowman, eds, TMS-AIME, Warrendale, PA, 1995, pp. 427-44.
105. D.A. Hughes and A. Godfrey: *Hot Deformation of Al Alloys II*, T.R. Bieler, L.A. Lalli, and S.R. MacEwan, eds. TMS-AIME, Warrendale, PA, 1998, pp. 23-36.
106. M. Richert, H.J. McQueen, and J. Richert: *Can. Metall. Q.*, 1998, vol. 37, pp. 449-57.
107. D. Kuhlmann-Wilsdorf: in *Work Hardening in Tension and Fatigue*, A.W. Thompson, ed., AIME, New York, NY, 1977, pp. 1-44.
108. D. Kuhlmann-Wilsdorf: *Phil. Mag.*, 1999, vol. A79, pp. 955-1048.
109. M. Meier, Q. Zhu, and W. Blum: *Z. Metallkd.*, 1993, vol. 84, p. 263.
110. M.E. Kassner, A.K. Miller, and O.D. Sherby: *Metall. Trans. A*, 1982, vol. A13, pp. 1977-86.
111. E. Evangelista, P. Mengucci, J. Bowles, and H.J. McQueen: *High Temp. Mater. Proc.*, 1993, vol. 12, pp. 57-66.
112. H.J. McQueen, N.D. Ryan, R. Zaripova, and K. Farkhutdinov: *Proc. 37th Mechanical Working and Steel Processing Conf.*, ISS-AIME, Warrendale, PA, 1996, pp. 883-94.
113. H.J. McQueen: *Proc. ICOTOM*, J.A. Szpunar, ed., NRC, Research Pub., Ottawa, 1999, vol. 12, pp. 836-41.
114. M.M. Myshlyaev, O.N. Senkov, and V.A. Likhachev: *Strength of Metals and Alloys, ICSMA 7*, H.J. McQueen, J.-P. Bailon, J.I. Dickson, J.J. Jonas, and M.G. Akben, eds., Pergamon Press, Oxford, United Kingdom, 1985, vol. 2, pp. 841-46.
115. C.S. Barrett and L.H. Levenson: *Trans. AIME*, 1940, vol. 137, pp. 112-27.
116. D. Kuhlmann-Wilsdorf: *Acta Mater.*, 1999, vol. 47, pp. 1697-1712.
117. B. Jaoul: *Ètude de la Plasticitè et Application aux Mètaux*, Dunod, Paris, 1965.
118. M. Wrobel, S. Dymeck, M. Blicharski, and S. Gorczyca: *Z. Metallkd.*, 1994, vol. 85, pp. 415-25.
119. A. Berger, P.J. Wilbrandt, and P. Haasen: *Acta Metall.*, 1983, vol. 31, pp. 1433-43.
120. W.R. Hibbard and C.G. Dunn: *Creep and Recovery*, ASM, Metals Park, OH, 1957, pp. 52-83.
121. R.D. Doherty, D.A. Hughes, F.J. Humphreys, J.J. Jonas, D. Juul-Jensen, M.E. Kassner (editor), W.E. King, T.R. McNelley, H.J. McQueen, and A.D. Rollett: *Mater. Sci. Eng.*, 1998, vol. 238, pp. 219-74.
122. M.C. Theyssier, B. Chenal, J.H. Driver, and N. Hansen: *Phys. Status Solid*, 1995, vol. A149, pp. 367-78.
123. S. Gourdet and F. Montheillet: *Mater. Sci. Eng.*, 2000, vol. A283, pp. 274-88.
124. S. Gourdet, E.V. Konopleva, H.J. McQueen, and F. Montheillet: *Mater. Sci. Forum*, 1996, vols. 217–222, pp. 441-46.
125. L. Gayard, M. Montheillet, and H.J. McQueen: *Proc. ICOTOM*, J.A.

Szpunar, ed., NRC Research Pub., Ottawa, 1999, vol. 12, pp. 878-83.

126. C.M. Sellars: *Phil. Trans. R. Soc.*, 1978, vol. A288, pp. 147-58.
127. T. Sakai and J.J. Jonas: *Acta Metall.*, 1984, vol. 32, pp. 189-209.
128. H.J. McQueen, E. Evangelista, and N.D. Ryan: in *Recrystallization ('90) in Metals and Materials*, T. Chandra, ed. AIME, Warrendale, PA, 1990, pp. 89-100.
129. H.J. McQueen and N.D. Ryan: in *Strip Casting, Hot and Cold Working of Stainless Steels*, N.D. Ryan, A. Brown, and H.J. McQueen, eds., TMS-CIM, Montreal, 1993, pp. 91-106 and 181-92.
130. Pho Bocher, J. Azar, B.L. Adams, and J.J. Jonas: *Proc. ITAP*, R.A. Schwarzer, ed., Clausthal, Germany, 1997, pp. 249-54.
131. H.J. McQueen: *Mater. Sci. Eng.*, 1987, vol. A101, pp. 149-60.
132. H.J. McQueen, E. Evangelista, N. Jin, and M.E. Kassner: in *Advances in Hot Deformation Textures and Microstructures*, J.J. Jonas, T.R. Bieler, and K.J. Bowman, eds., TMS-AIME, Warrendale, PA, 1993, pp. 251-66.
133. F.J. Humphreys and P. Kalu: *Acta Metall.*, 1987, vol. 35, pp. 2815-29.
134. B.M. Watts, M.J. Stowell, B.L. Baikie, and D.G. Owen: *Met. Sci.*, 1976, vol. 10, pp. 189-97 and 198-205.
135. R.H. Bricknell and J.W. Edington: *Acta Metall.*, 1979, vol. 27, pp. 1303-11.
136. S.J. Hales, T.R. McNelley, and H.J. McQueen: *Metall. Trans.*, 1991, vol. 22A, pp. 1037-47.
137. H.J. McQueen, W. Blum, S. Straub, and M.E. Kassner: *Scripta Metall. Mater.*, 1993, vol. 28, pp. 1299-1304.
138. N.J. Grant and A.R. Chaudhuri: in *Deformation and Fracture at Elevated Temperatures*, N.J. Grant, and A.W. Mullendare, eds., MIT Press, Cambridge, MA, 1965, pp. 165-211.
139. R.W. Guard and W.R. Hibbard: *Trans AIME*, 1956, vol. 206, pp. 195-98.
140. P.B. Hirsch: *Progress in Metal Physics*, Pergamon Press, London, 1957, vol. 6, pp. 261-339.
141. P.A. Beck and P.R. Sperry: *J. Appl. Phys.*, 1950, vol. 21, p. 150.
142. H.J. McQueen: *Defects Fracture and Fatigue*, G. Sih and W. Provan, eds., Martinus Nichoff Pub., The Hague, 1983, pp. 459-71.
143. H.J. McQueen, J. Sankar, and S. Fulop: *Mechanical Behavior of Materials*, (ICM 3), Pergamon Press, Oxford, United Kingdom, 1979, vol. 2, pp. 675-84.
144. F. Garofalo, C. Richmond, W.F. Domus, and V. Von Gemingen: *Joint Int. Conf. on Creep*, Institute of Mechanical Engineers, London, 1963, pp. I31-39.
145. M.E. Kassner, N.Q. Nguyen, G.A. Henshall, and H.J. McQueen: *Mater. Sci. Eng.*, 1991, vol. A132, pp. 97-105.
146. M.F. Ashby: *Frontiers in Materials Science*, L.E. Murr, and C. Stein, eds., Marcel Dekker, New York, NY, 1976, pp. 391-417.
147. E.E. White: *Rev. Metall.*, 1966, vol. 63, pp. 991-98.
148. E. Shapiro and G.E. Dieter: *Metall. Trans.*, 1970, vol. 1, pp. 1711-19; 1971, vol. 2, pp. 1385-91.
149. H.J. McQueen, J. Bowles, and N.D. Ryan: *Microstr. Sci.*, 1989, vol. 17, pp. 357-73.

150. C.M. Sellars: *Creep Strength in Steel and High Temperature Alloys*, The Metals Society, London, 1974, pp. 20-30.
151. C.M. Young and O.D. Sherby: *Simulation of Hot Forming Operations by Means of Torsion Testing*, AFML-TR-69-294, Stanford University, Palo Alto, CA, 1969.
152. S. Fulop and H.J. McQueen: *Super Alloys Processing*, Proc. 2nd Int. Conf., AIME, Warrendale, PA, 1972, pp. H-1-H-21.
153. J.M. Oblak and W.A. Owezarski: *Metall. Trans.*, 1972, vol. 3, pp. 617-26.
154. J.J. Jonas and I. Weiss: *Met. Sci.*, 1979, vol. 13, pp. 238-45.
155. M.G. Akben, I. Weiss, and J.J. Jonas: *Acta Metall.*, 1981, vol. 29, pp. 111-221.
156. H.J. McQueen and C.A.C. Imbert: *Deformation, Processing and Properties of Structural Materials* (Honoring O.D. Sherby) E.M. Taleff, C.K. Syn, and D.R. Lesuer, eds., TMS-AIME, Warrendale, PA, 2000, pp. 79-92.
157. H.J. McQueen, H. Chia, and E.A. Starke: in *Microstructural Control in Al Alloy Processing*, H. Chia, and H.J. McQueen, eds., TMS-AIME, Warrendale, PA, 1985, pp. 1-18.
158. E. Cerri, E. Evangelista, A. Forcellese, and H.J. McQueen: *Mater. Sci. Eng.*, 1995, vol. A197, pp. 181-98.
159. H.J. McQueen: in *Hot Deformation of Aluminum Alloys*, T.G. Langdon and H.D. Merchant, eds., TMS-AIME, Warrendale, PA, 1991, pp. 105-20.
160. Hsun Hu: *Recovery, Recrystallization of Metals*, Gordon and New York, Breach, NY, 1963, pp. 311-78.
161. T. Hasegawa, T. Yakou, and U.F. Kocks: *Acta Metall.*, 1982, vol. 30, pp. 235-43.
162. N.D. Ryan and H.J. McQueen: *Can. Met. Q.*, 1991, vol. 30, pp. 113-24.
163. N.D. Ryan and H.J. McQueen: *J. Mater. Proc. Technol.*, 1993, vol. 36, pp. 103-23.
164. R.A. Petkovic, M.J. Luton, and J.J. Jonas: in *Hot Deformation of Austenite*, J.B. Ballance, ed., AIME, New York, NY, 1977, pp. 68-85.
165. R. Chadwick: *Met. Rev.*, 1959, vol. 4, pp. 189-255.
166. V.M. Khlestov, E.V. Konopleva, and H.J. McQueen: *Can. Metall. Q.*, 1998, vol. 37, pp. 75-89.
167. E.V. Konopleva, H.J. McQueen, and V.M. Khlestov: *Thermo-mechanical Processing of Steel*, Institute of Materials, London, 2000, vol. 1, pp. 287-96.
168. E.V. Konopleva and H.J. McQueen: *Hot Workability of Steels and Light Alloys-Composites*, TMS-CIM, Montreal, 1996, pp. 557-68.
169. J.J. Irani and P.R. Taylor: *Deformation under Hot Working Conditions*, Iron and Steel Institute, London, 1968, pp. 83-96.
170. H.J. McQueen, A. Hopkins, V. Jain, E.V. Konopleva, and P. Sakaris: *Al Alloys, Physical and Mechanical Properties*, ICAA/4, Atlanta, GA, T. Sanders and E.A. Starke, eds., Georgia Institute of Technology, Atlanta, GA, 1994, vol. 2, pp. 250-57.
171. N.D. Ryan and H.J. McQueen: *Can. Met. O.*, 1990, vol. 29, pp. 147-62.
172. P. Wouters, B. Verlinden, H.J. McQueen, and E. Aernoudt: *Mater. Sci. Eng.*, 1990, vol. A123, pp. 229-37 and 239-45.
173. F. Bardi, M. Cabibbo, and S. Spigarelli: *Mater. Sci. Eng.*, 2001, in press.